NASA TECHNICAL NOTE

NASA TN D-7214

NASA TN D-7214

ANALYSIS OF TEMPERATURE-DEPENDENT NEUTRON TRANSMISSION AND SELF-INDICATION MEASUREMENTS ON TANTALUM AT 2-keV NEUTRON ENERGY

by Thor T. Semler

Lewis Research Center
Cleveland, Ohio 44135

NATIONAL AERONAUTICS AND SPACE ADMINISTRATION • WASHINGTON, D. C. • MARCH 1973

1. Report No.	2. Government Accession No.	3. Recipient's Catalog No.
NASA TN D-7214		

4. Title and Subtitle	5. Report Date
ANALYSIS OF TEMPERATURE-DEPENDENT NEUTRON TRANSMISSION AND SELF-INDICATION MEASUREMENTS ON TANTALUM AT 2-keV NEUTRON ENERGY	March 1973
	6. Performing Organization Code

7. Author(s)	8. Performing Organization Report No
Thor T. Semler	E-7282
	10 Work Unit No
	503-25

9. Performing Organization Name and Address	11. Contract or Grant No
Lewis Research Center National Aeronautics and Space Administration Cleveland, Ohio 44135	

12 Sponsoring Agency Name and Address	13. Type of Report and Period Covered
National Aeronautics and Space Administration Washington, D.C. 20546	Technical Note
	14. Sponsoring Agency Code

15. Supplementary Notes

16. Abstract

The method of pseudo-resonance cross sections is used to analyze published temperature-dependent neutron transmission and self-indication measurements on tantalum in the unresolved region. In the energy region analyzed, 1825.0 to 2017.0 eV, a direct application of the pseudo-resonance approach using a customary average strength function will not provide effective cross sections which fit the measured cross section behavior. Rather a local value of the strength function is required, and a set of resonances which model the measured behavior of the effective cross sections is derived. This derived set of resonance parameters adequately represents the observed resonance behavior in this local energy region. Similar analyses for the measurements in other unresolved energy regions are necessary to obtain local resonance parameters for improved reactor calculations. This study suggests that Doppler coefficients calculated by sampling from grand average statistical distributions over the entire unresolved resonance region can be in error, since significant local variations in the statistical distributions are not taken into consideration.

17. Key Words (Suggested by Author(s))	18. Distribution Statement
Tantalum; Fast reactor safety; Fast neutron physics; Doppler effect; Neutron spectroscopy; Pseudo resonance; Statistical distributions; Unresolved resonance; Neutron transmission	Unclassified - unlimited

19 Security Classif. (of this report)	20 Security Classif. (of this page)	21 No. of Pages	22 Price*
Unclassified	Unclassified	46	$3.00

* For sale by the National Technical Information Service, Springfield, Virginia 22151

ANALYSIS OF TEMPERATURE-DEPENDENT NEUTRON TRANSMISSION AND SELF-INDICATION MEASUREMENTS ON TANTALUM AT 2-keV NEUTRON ENERGY

by Thor T. Semler

Lewis Research Center

SUMMARY

The method of pseudo-resonance cross sections is used to analyze an experiment which measured the temperature-dependent change in neutron transmission and self-indication ratio in the unresolved keV neutron energy region. The self-indication experiments consist of energy- and temperature-dependent measurements of transmission samples of tantalum followed directly by a capture sample of tantalum in a gamma-ray detector. The self-indication ratio is then the ratio of the number of captures in the capture sample when the transmission sample is in the beam to the number of captures when it is out of the beam.

The observed transmission and self-indication ratio have been converted into effective total cross sections for the various samples. These show variations with energy due to local variations in the strength of resonances. At 2 keV the energy resolution of the tantalum experiment is 192.0 eV and contains on the average about 45 resonance levels. A general technique based on pseudo-resonance parameters is described that is used to extract local strength functions and a consistent set of resonance parameters. For the 2-keV experiment a 0.7-meV value of the reduced scattering width $\overline{\Gamma}_n^0$ and a potential cross section σ_{pot} of 9.5 barns fitted all six of the temperature-dependent transmission experiments and four out of six temperature-dependent self-indication experiments.

Finally, a set of resonance parameters which adequately represent the temperature-dependent behavior of the measured effective cross sections at 2 keV is derived. This set is suitable for reactor calculations in this energy region. Similar analyses for the measurements in other unresolved energy regions are necessary to obtain local resonance parameters for improved reactor Doppler calculations.

An evaluation of another published experiment using a scandium-filtered beam of neutrons upon tantalum is presented. The precision of this experiment was unfortunately degraded by the presence of neutrons streaming down the duct containing a scandium filter. However, by using the measured scandium-filtered beam spectrum and recently measured cross sections for tantalum, some evidence is adduced for the adequacy of the pseudo-resonance approach for the analysis of this experiment as well.

INTRODUCTION

The Doppler effect is a measure of the change of effective neutron cross section with temperature and is of major importance to the design and safety considerations for fast reactors. A strong negative Doppler effect implies an increase in neutron capture with increasing reactor temperature and is desirable to limit prompt supercritical excursions. Thus, an accurate estimate of the Doppler effect of reactor materials is needed for fast-reactor design.

Temperature-dependent continuous neutron cross sections, in the energy region where individual resonances are unresolved in cross section measurements, may be used to calculate neutron Doppler effects in such regions. If it is assumed that the statistical distributions of resonance parameters obtained from analysis of the resolved resonance levels measured at neutron energies, from 0 to about 1 keV, are representative of the statistical distributions at the higher unresolved energies, it is possible to sample from these distributions and generate "pseudo" resonance parameters (refs. 1 to 4). These pseudo-resonance parameters may then be used to compute energy- and temperature-dependent cross sections from which have been evaluated the Doppler effect (ref. 1), the average capture cross sections (ref. 2), or the effects of overlapping fission resonances (ref. 3). Rarely have such calculations been checked against experiments which measure the variation of the cross section as a function of temperature and energy in the unresolved resonance region.

Two experiments have been performed which measured the change in neutron transmission of tantalum as a function of sample temperature (refs. 5 to 7). It was shown by Byoun, Block, and Semler (ref. 5, hereinafter referred to as RPI 1971) that the results of neutron transmission and self-indication experiments on tantalum at room temperature could be analyzed by the method of pseudo-resonance chains. However, an earlier attempt to fit the experimentally measured change in effective total cross section at 2 keV due to temperature by pseudo-resonance parameters was unsuccessful (refs. 6 and 7, hereinafter referred to as INC 1968).

This report demonstrates a use of the method of pseudo-resonance chains to elicit a set of resonance parameters which reproduce the temperature-dependent RPI 1971 measurements at 2 keV and are suitable for reactor calculations in this region. As the average effective total cross section of tantalum shows considerable structure in the unresolved region (see fig. 5), it is clear that there are significant differences in the local values of the strength function. Thus, a general method which allows extraction of the local strength functions and consistent resonance parameters is used. The region at 2 keV has been chosen to illustrate this technique since there appears to be a significant "window" in the total cross section which should provide a severe test of the method and since there exist other temperature-dependent data in this energy region (ref. 6).

This method, presently applied to tantalum, should be generally applicable to energy regions where the p-wave and inelastic cross sections are small or are accurately known. A discussion of the average resonance parameters measured for tantalum and used as constraints in the analysis is included. A brief critique of the INC 1968 experiment is also included.

METHOD OF PSEUDO-RESONANCE CHAINS

The assumption has been generally made that the statistical distributions found in the resolved resonance region are valid at higher neutron energies (refs. 1, 2, and 4). These distributions of resonance parameters are used to generate a set of resonance parameters in the unresolved resonance region. The code DAISY (ref. 8) allows one to generate chains of pseudo-resonance parameters in the unresolved resonance region which preserve the correct average values as well as accurately represent the correct distribution functions.

Wigner Level Spacing Distribution

The level spacing between two neutron resonances, of like J and ℓ, follows a probability distribution of the form

$$\left.\begin{aligned} p(x) &= \frac{\pi}{2} x \exp\left(-\frac{\pi}{4} x^2\right) \qquad x \geq 0 \\ p(x) &= 0 \qquad\qquad\qquad\qquad\quad x < 0 \end{aligned}\right\} \tag{1}$$

where J is the spin quantum number of the compound nucleus formed by the target nucleus and the neutron, ℓ is the angular momentum of the bombarding neutron with respect to the target nucleus, and x is a normalized dimensionless level spacing or

$$x = \frac{S}{\overline{D}_J} \tag{2}$$

where S is the nearest neighbor level spacing in eV and $\overline{D}_J$ is the J-state average level spacing in eV.

When the Wigner level spacing distribution is written as equation (1), the expectation of x is 1. In order to sample X, a level spacing, from this normalized Wigner

distribution, we form the functional mapping (eq. (3))

$$R_n = \int_0^X p(x)\, dx \tag{3}$$

where R_n is a random number uniformly distributed on the interval (0, 1) which gives

$$R_n = \frac{\pi}{2} \int_0^X x \exp\left(-\frac{\pi}{2} x^2\right) dx \tag{4}$$

Solving for X and substituting R_n for $(1 - R_n)$, we obtain

$$X = \frac{2}{\sqrt{\pi}} \sqrt{-\ln (R_n)} \tag{5}$$

We may now easily gain the correct J-state level spacing by multiplying X by $\overline{D}_J$, the J-state average level spacing.

Level Width Distribution of Porter and Thomas

The variation of the reduced scattering widths Γ_n^0 is found to follow a χ^2 probability distribution function with one degree of freedom for s-wave ($l = 0$) resonances, while two degrees of freedom have been suggested for p-wave ($l = 1$) resonances; that is,

$$\Gamma_n^0 = E_0^{1/2} \nu_l \Gamma_n \tag{6}$$

where E_0 is the resonance energy in eV, ν_l is the penetrability factor, and Γ_n is the scattering width associated with the Breit-Wigner formula. The distribution of the dimensionless reduced scattering widths

$$y = \frac{\Gamma_n^0}{\overline{\Gamma}_n^0} \tag{7}$$

is found to be of the form

$$P_m(y) = \frac{m}{2\Gamma\left(\frac{m}{2}\right)}\left(\frac{my}{2}\right)^{(m/2)-1}\exp\left(\frac{-my}{2}\right) \qquad (8)$$

where the number of degrees of freedom m is equal to 1 for s-wave resonances and 2 for p-wave resonances. This analysis will be restricted to s-wave resonances since the strength function and penetrability for p-wave neutrons at 2 keV for tantalum are quite small. This is the distribution of Porter and Thomas for scattering widths.

It can be shown that the problem of sampling an element from a χ^2 distribution with m degrees of freedom can be reduced to the problem of sampling m random values drawn from a normal distribution of mean 0 and variance 1. That is, if the sequence

$$Y_1, Y_2, Y_3, Y_4, \ldots, Y_r, \ldots$$

is composed of values selected from a normal distribution of unit variance and mean 0, the sequence of transformed random variables

$$Y_1^2, Y_2^2, Y_3^2, Y_4^2, \ldots, Y_r^2, \ldots$$

has a χ^2 distribution of one degree of freedom.

Once a series of E_0's, or resonance energies, have been generated, we can sample from the appropriate χ^2 distribution; the value of Γ_n associated with the n^{th} E_0 is then

$$\Gamma_n(E_n) = E_0^{1/2}\overline{\Gamma}_n^0 Y_n^2 \nu_0 \qquad \text{(s-wave)} \qquad (9)$$

where $\nu_0 = 1$.

Program DAISY

The program DAISY (ref. 8) is given the average level spacing for a resonance chain and the average reduced scattering width. It then generates many pseudo-resonance chains or sets of resonance parameters (as many as 9999 chains of at most 5000 resonances) with level spacings chosen from Wigner's level spacing distribution and scattering widths chosen from the distribution of Porter and Thomas as described in the preceding section. The code then rejects those chains whose averages are beyond

the limits associated with a preselected probability level. This allows us to select a confidence probability level, say 95 percent, and to reject a chain if it does not approximate the average level spacing and/or the average scattering width better than 95 percent of all chains generated. This process limits the allowable variation in the average cross sections computed from such selected chains. The code then chooses, from these selected chains, that particular chain whose individual parameters best fit the theoretical distribution functions. Either the Kolmogorov-Smirnoff or χ^2 tests for goodness of fit are used for such a selection of this best chain. Thus, the chain finally chosen by the program DAISY shall have the correct average values, and the distribution of the chain's individual parameters will most closely resemble their theoretical distribution functions.

CROSS SECTIONS AND RESONANCE PARAMETERS FOR TANTALUM

In order to use the method of pseudo-resonance parameter chains, we must have values of the average reduced neutron width $\overline{\Gamma}_n^0$, the average level spacing $\overline{D}$, the potential scattering cross section σ_{pot}, and the average capture width $\overline{\Gamma}_\gamma$. Certain of these parameters will be varied parametrically as part of the analysis. However, accurate values of the averages and their associated experimental errors are necessary as they are used as constraints on the final results of the analysis. These parameters may be obtained from measurements in the resolved resonance region. The following section gives the source of the parameters used for tantalum, along with a brief evaluation of their accuracy. The average values and their associated accuracy chosen for the present analysis are shown.

Potential Scattering Cross Section

Two experimental techniques which allow the determination of the potential scattering cross section are the bright-line technique and the average-cross-section method. In the "bright-line" technique, the total cross section is measured by a high-resolution crystal spectrometer near a prominent resonance; for tantalum the 4.28-eV resonance was used. The measured values are fitted by a resolution- and Doppler-corrected theoretical cross-section curve. The parameters of the best-fitting theoretical curve are then reported as the resonance parameters for that particular resonance. Since both a resonance peak and a resonance wing analysis are performed, the potential cross section may also be extracted. In 1956, Wood, using the (BNL) crystal spectrometer, reported high-resolution measurements on four sample thicknesses of tantalum (ref. 9).

TABLE I. - COMPARISON OF WOOD (1956) RESONANCE PARAMETERS OF 4.28-eV RESONANCE IN ^{181}Ta WITH LATER MEASUREMENTS

Parameter	Source			
	Wood (1956), ref. 9	Evans (1958), ref. 10	Doĭl'nitsyn (1961), ref. 11 (a)	Stolovy (1963), ref. 12
Spin quantum number, J	4	4	(4)	4
Statistical factor, g	9/16	9/16	(9/16)	9/16
Scattering width, Γ_n, meV	3.9±0.6	3.6±0 1	(3.6±0.1)	----
Capture width, Γ_γ, meV	49±6	62±2.6	51±5	----
Total width, Γ, meV	53±5	66±2.7	56±5	----
Resonance energy, E, eV	4.282±0.008	4.28±0.01	4.28±0.01	----
Potential cross section, σ_{pot}, barns	7.0±1 0	---------	---------	----

[a]Only $2g\Gamma_n$ reported, thus the parameters in parentheses were derived by assuming J = 4.

the parameters extracted by Wood are shown in table I. As can be seen, later experiments (refs. 10 to 12) have confirmed the spin assignment J of the 4.28-eV level. It should also be noted that later experiments have obtained somewhat higher values of the total width Γ, indicating the experimental value reported of $\sigma_{pot} = 7.0 \pm 1.0$ barns may be high.

A second technique for the measurement of the potential cross section is the so-called "average-cross-section method." If the transmission of neutrons averaged over many resonances, in the unresolved region, is plotted as a function of sample thickness, the slope for thin samples is proportional to the s-wave strength function. However, for thick samples the average transmission is

$$\overline{T} = T_P\left(1 - 2\sqrt{2}\,\pi\lambda\bar{}\,\frac{\Gamma_n}{D}\sqrt{nt}\right) \tag{10}$$

if it is assumed that the statistical factor g equals 1/2, $\Gamma_n = \Gamma$, and resonance-resonance interference terms cancel. In equation (10), T_P, is the transmission corresponding to a potential cross section σ_{pot} only, D is the average spacing for levels of a single spin state, nt is the sample thickness in centimeters, and $\lambda\bar{}$ is the neutron wavelength divided by 2π. Taking the logarithm, differentiating with respect to nt and neglecting higher order terms yields equation (11).

$$\frac{d}{d\,nt}(\ln \overline{T}) = \left[\sigma_{pot} + \sqrt{2}\,\pi\left(\frac{\lambda\bar{}}{\sqrt{nt}}\right)\frac{\Gamma_n}{D}\right] \tag{11}$$

Thus, for thick samples the slope of $\ln \overline{T}$ as a function of nt is asymptotic to σ_{pot}.

In an analysis of tantalum neutron transmission experiments, Seth, Hughes, Zimmerman, and Garth (ref. 13) in 1958 selected four "typical" resonances and computed their cross section, including interference effects and Doppler broadening. Then average transmissions were computed for various sample thicknesses, and reasonable agreement with experiment was obtained for a $\sigma_{pot} = 8.5 \pm 1.0$ barns.

Using the same technique, Divadeenam (ref. 14) in 1967 reported an extremely small value of the potential radius, which would imply a potential cross section of 4.80 barns. However, a very high value of the s-wave strength function S_0 was also reported. The Divadeenam value of S_0 for tantalum reported was 3.1×10^{-4} (ref. 14). This may be compared with the S_0-value reported by Desjardins, Rosen, Havens, and Rainwater of 1.84×10^{-4} obtained from the individual measurement of 62 separated resonances (ref. 15). Thus, the Divadeenam value for the potential cross section may be somewhat suspect.

The value for the potential cross section chosen for the present analysis is 8.5 (+1.0, -2.5) barns. The negative value of the error is chosen to reflect the lower value of Wood (ref. 9).

Average Level Spacing

The average level spacing $\overline{D}$ of tantalum is determined by measuring the energies of individual resonances, subtracting the lowest resonance energy from the highest resonance energy measured, and dividing by one less than the number of resonances, or

$$\overline{D} = \frac{E_n - E_1}{n - 1} \tag{12}$$

where E_n is the resonance energy of the n^{th} resonance measured from the first resonance energy E_1. A value of $\overline{D}$ for tantalum of 4.5 eV was reported by Garg, Rainwater, and Havens in 1966 (refs. 16 and 17). These measurements extended from about 30 eV to over 1300 eV and comprised over 300 neutron resonance energies. Figure 1 shows the cumulative probability distribution of the level spacings measured experimentally compared to the theoretical cumulative probability distribution of two uncorrelated Wigner level spacing distributions. The cumulative probability distribution function F(s) of two Wigner single-species level spacing distributions which have been superimposed on one another is given by the following formula:

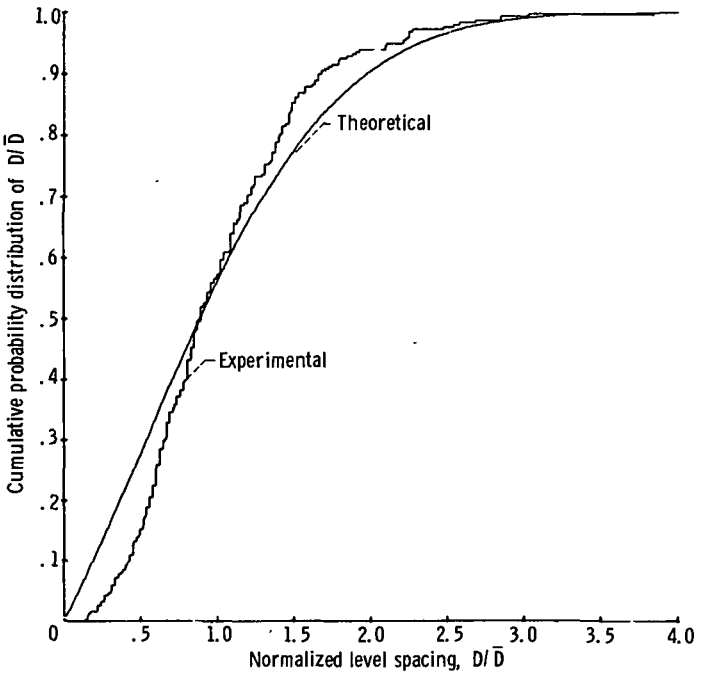

Figure 1. - Cumulative probability distribution of normalized level spacing compared to Wigner level spacing distribution for two spin species - for first 300 level spacings reported in reference 17. Number of level spacings, 300; ratio of average level spacings for two spin species, 1.286; average level spacing of first 300 level spacings, 4.526 eV; energy E_0 of last resonance used in average and display, 1362.2 eV.

$$F(s) = \int_0^s P(s)\,ds = 1 - \frac{1}{1+k}\left\{k \exp\left(\frac{-a^2}{2}\right)\left[1 - 2\,\mathrm{erf}\,(b)\right] + \exp\left(\frac{-b^2}{2}\right)\left[1 - 2\,\mathrm{erf}\,(a)\right]\right\} \tag{13}$$

where k is the ratio of the average spacings of the two individual Wigner single-specie distributions ($k = D_2/D_1$) and s is the spacing.

$$a = \left(\frac{\pi}{2}\right)^{1/2} \frac{s}{D_1}$$

$$b = \left(\frac{\pi}{2}\right)^{1/2} \frac{s}{D_2}$$

$$\mathrm{erf}\,(x) \equiv \frac{1}{\sqrt{2\pi}} \int_0^x \exp\left(\frac{-y^2}{2}\right) dy$$

If a $(2J + 1)$ level density obtains, 7/16 of the levels should have $J = 3$ and 9/16 of the levels $J = 4$, where J is the spin of the compound nucleus. Thus, the appropriate value of k, or D_2/D_1, is 9/7 or 1.286. As can be seen in figure 1 there is an excess of measured level spacings in the region between $\overline{D}$ and about 2.5 $\overline{D}$, and a deficit of measured level spacings in the region 0 to $\overline{D}$. This indicates that if the Wigner model applies, many closely spaced resonances have not been resolved in the experiment of references 16 and 17. The fit of the experimental data to the theoretical curve is nearly the same for $k = 1$. The fit is somewhat improved for very large (or very small) k, when the theoretical curve approximates the single-species Wigner cumulative distribution. However, in the low-energy region, from about 0 eV to about 300 eV, where few if any levels are missed experimentally, the fit of experimental data to the expected theoretical curve is quite good (see fig. 2 and appendix A); perhaps only three levels are missing. Using this low-energy, portion $\overline{D}$ is estimated to be 4.3 ± 0.2 eV.

Average Reduced Scattering Width

The strength function S_0 is generally defined as the ratio of average reduced scat-

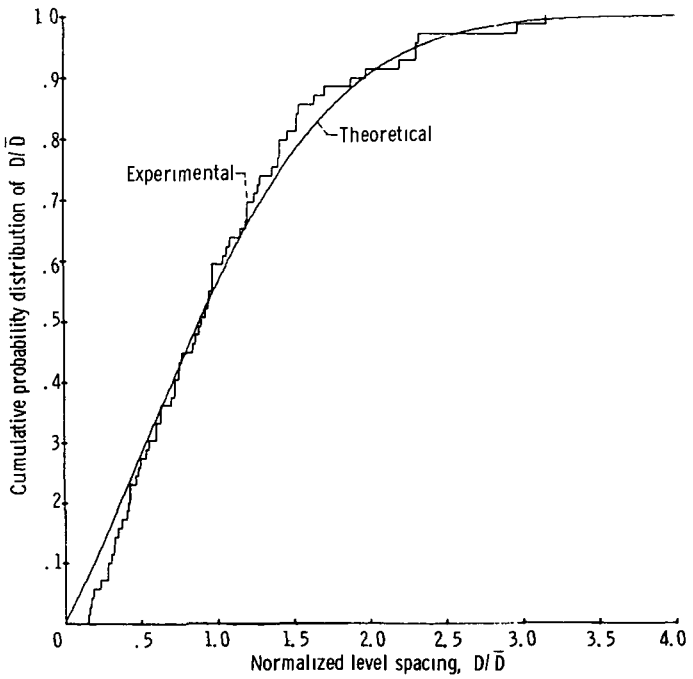

Figure 2. - Cumulative probability distribution of normalized level spacing compared to Wigner level spacing distribution for two spin species - for first 69 level spacings reported in reference 17. Number of level spacings, 69; ratio of average level spacings for two spin species, 1.286; average level spacing of first 69 level spacings, 4.344 eV; energy E_0 of last resonance used in average and display, 304.0 eV.

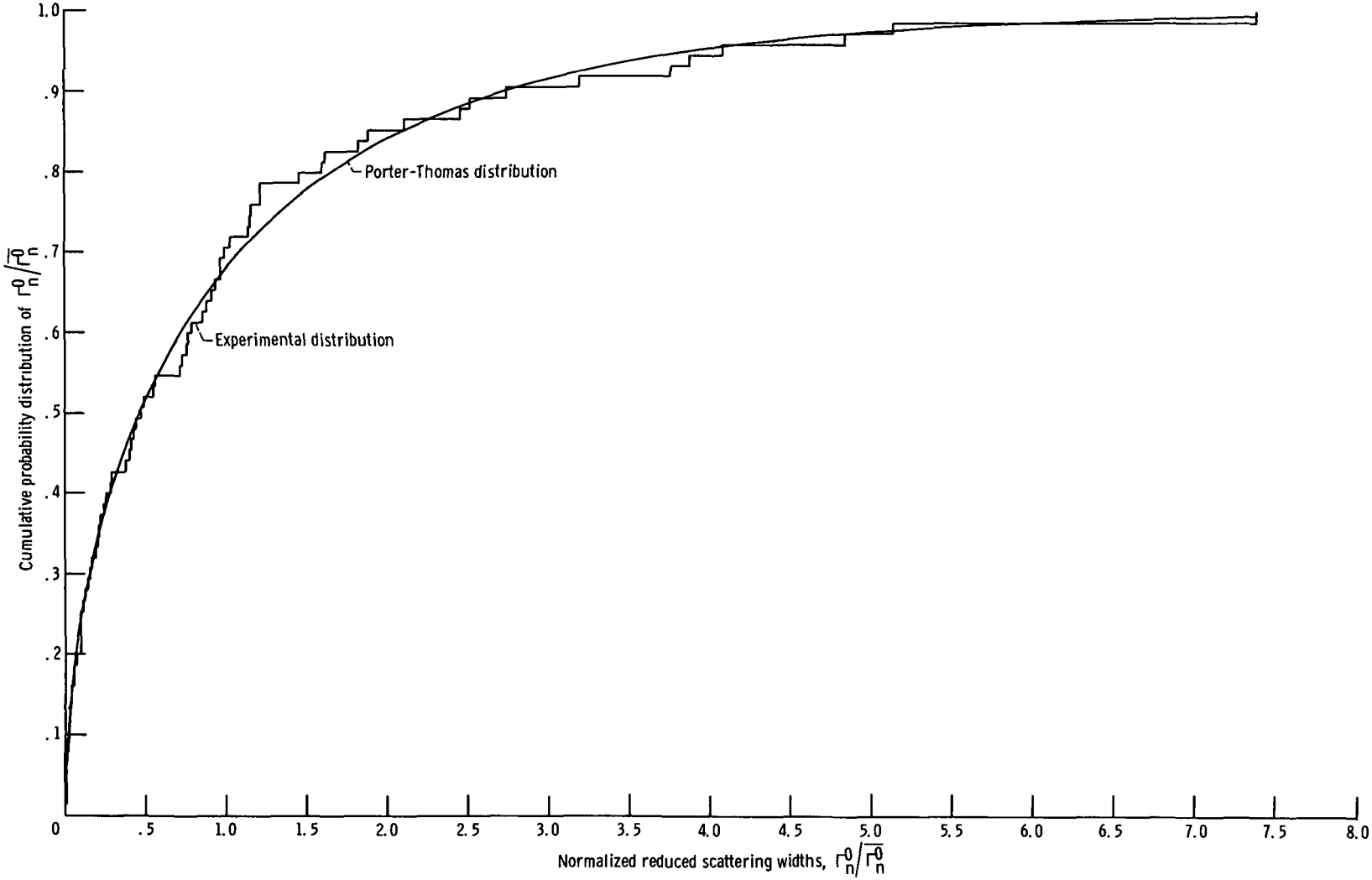

Figure 3. - Cumulative probability distribution of normalized reduced scattering widths compared to Porter-Thomas distribution of reduced scattering widths - for 75 widths reported in reference 17.

tering width $\overline{\Gamma}_n^0$ for a particular J-state over the average level spacing for that particular J-state. We assume that $\overline{\Gamma}_n^0(J = 3) = \overline{\Gamma}_n^0(J = 4)$; and figure 3, since there is good agreement between the theoretical distribution and the experimentally measured distribution, indicates this to be a reasonable assumption for tantalum. If we further assume $\overline{D}(J = 3) = \overline{D}(J = 4) = 2\overline{D}$, we may easily obtain the value of $\overline{\Gamma}_n^0$ by the following equation:

$$\overline{\Gamma}_n^0 = 2\overline{D}S_0 \tag{14}$$

Two rather different means have been used to measure the s-wave strength function. One technique has been to measure the average energy-dependent behavior of the total cross section, to apply self-shielding corrections, and then to choose the s-wave strength function which best fits the resulting total cross-section curve. The other technique has been to measure the individual Γ_n's of resolved, low-energy resonances and then to determine the strength function directly from the inferred values of Γ_n^0 or $2g\Gamma_n^0$. Table II gives a summary of measurements of the s-wave strength function (refs. 14, 15, and 18 to 21), along with the value of $\overline{\Gamma}_n^0$ obtained by use of equation (14).

A value of $\overline{\Gamma}_n^0$ near the mean of the values shown in table II has been chosen, and an error has been chosen to cover the range of the experiments. A value of $\overline{\Gamma}_n^0 = 2.0$ $(+0.9, -1.2)$ meV has been chosen.

Average Capture Width

The average capture width $\overline{\Gamma}_\gamma$ is expected to be distributed as χ^2 with a large number of degrees of freedom and should be well approximated by the normal distribution. The capture width has been measured for 26 resonances of tantalum. The weighted mean of these individual Γ_γ's has been reported as 60 meV (ref. 15). However, only relatively large values of Γ_γ are measured since Γ_γ must be larger than or at least of the order of Γ_n to be measured. Hence, the distribution of measured Γ_γ's

TABLE II - MEASURED s-WAVE STRENGTH FUNCTIONS FOR TANTALUM AND ASSOCIATED SOURCE

	Source					
	Simpson (1958), ref 18	Desjardins (1960), ref 15 (a)	Seth (1964), ref 19	Divadeenam (1967), ref 14	Frike (1971), ref 20	Dilg and Vonach (1971), ref 21
s-Wave strength function	(2 00±0 24)×10^{-4}	(1 84±0 34)×10^{-4}	(2 50±0 50)×10^{-4}	3 1×10^{-4}	(2 2±1 2)×10^{-4}	2 6±0 5
Average reduced scattering width, $\overline{\Gamma}_n^0$, meV	1 72±0 20	1 58±0 29	1 58±0 29	2 67	1 89±1 03	2 24±0 43

[a] S_0 determined from individual resonances

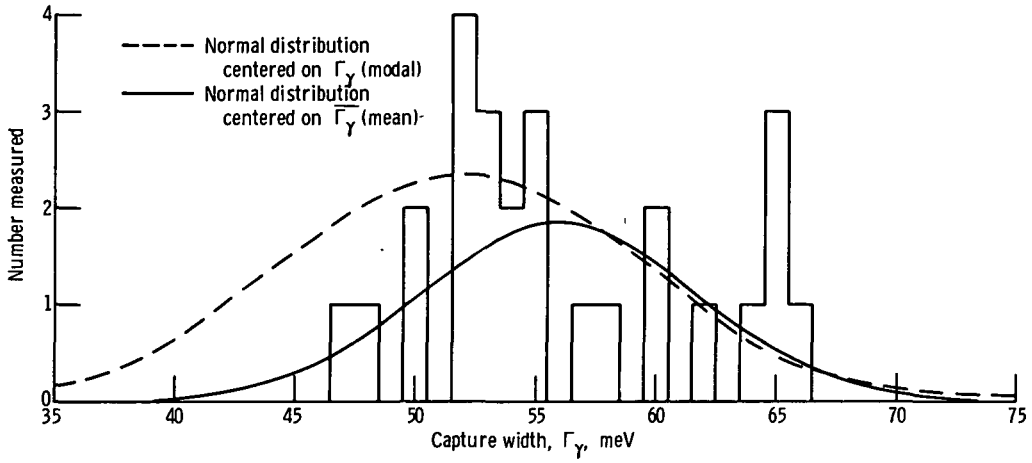

Figure 4. - Distribution of measured capture widths of tantalum, along with normal distributions centered on mean and mode of measured distribution (refs. 15 and 17). Modal value is taken as more representative of mean of capture widths of tantalum (see text). Measured values are shown as histograms.

is not the same as the expected distribution of Γ_γ's but is biased toward higher values of Γ_γ, figure 4. Thus, a measure of central tendency other than the mean should be chosen in order to eliminate some of the bias. Here the mode, or most probable value, has been chosen as a less biased estimator of the true value of $\overline{\Gamma}_\gamma$. A value of $\overline{\Gamma}_\gamma$ = 52±7.5 meV is thus obtained. Normal approximations to the distribution of Γ_γ obtained by using both the mean and mode as the measure of central tendency are shown in figure 4.

Nominal Values of Parameters

The nominal values chosen for the average resonance parameters for tantalum are as follows:

(1) Potential cross section, σ_{pot}, 8.5 (+1.0, -2.5) barns

(2) Average level spacing, $\overline{D}$, 4.3±0.2 eV

(3) Average reduced scattering width, $\overline{\Gamma}^0_n$, 2.0 (+0.9, -1.2) meV

(4) Average capture width, $\overline{\Gamma}_\gamma$, 52±7.5 meV

These average values are used as initial values for the analysis and their associated errors are used as constraints of the analysis.

DESCRIPTION OF EXPERIMENTS AND ANALYSIS

Description of Experiments

Brief descriptions of the two experiments on tantalum at 2-keV neutron energy follow. If the reader is interested in more experimental detail, the original reports should be consulted.

Rensselaer Polytechnic Institute (RPI) experiment - 1971. - A series of neutron transmission and self-indication experiments were performed on tantalum below 100 keV (transmission results in fig. 5) to study the effects of resonance self-shielding in the unresolved neutron energy range (ref. 5). Only those results about 2-keV neutron energy, shown in table III, are considered in this report.

Room-temperature (295 K), high-temperature (1073 K), and low-temperature (77 K) transmission and self-indication experiments were carried out with sample thicknesses of 0.0278 and 0.0549 atoms per barn. These samples provided significant temperature variations of the effective cross section and correspond to nominal tantalum thicknesses of 0.5 and 1.0 centimeters.

Likewise, self-indication ratios (SIR) were measured as a function of neutron energy and the temperature of the transmission sample. The self-indication experiment consists of a transmission sample of tantalum, which may be heated or cooled, and a detector sample of tantalum which is inside the RPI 1.25-meter liquid scintillator capture

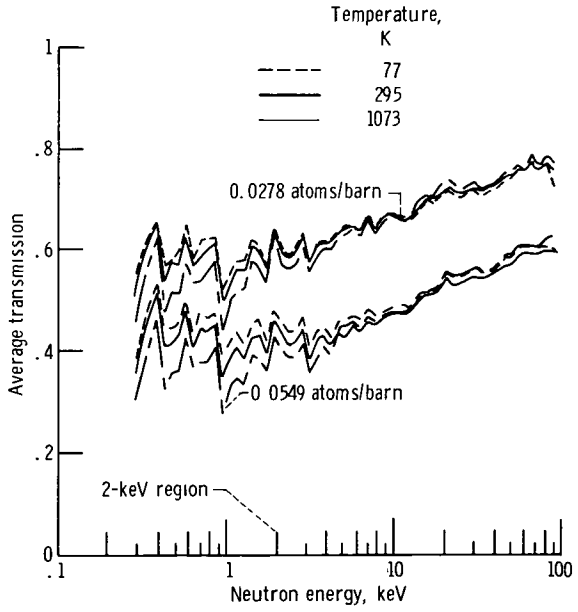

Figure 5 - Average transmission over energy region 300 eV to 100 keV for two samples of tantalum. (Data from ref. 5, RPI 1971)

TABLE III. - RPI 1971 RESULTS AT APPROXIMATELY 2keV FOR TANTALUM IN TRANSMISSION AND SELF-INDICATION (1825.0 TO 2017.0 eV)

[Errors shown are three-sigma limits.]

Slab thickness, cm	Effective average total cross section, $\bar{\sigma}_t$, barns, at -		
	77 K	295 K	1073 K
Transmission			
0.5	15.25±1.14	15.67±0.83	16.59±1.08
1.0	13.13±0.52	13.90±0.41	15.09±0.58
Self-indication			
0.5	28.90±2.74	29.98±1.23	30.72±2.20
1.0	25.31±1.03	26.41±0.65	26.06±1.27

detector. The SIR's are then the ratio of captures in the detector sample with the transmission sample in the neutron beam to those with the transmission sample out of the beam. For these experiments the detector sample, which is down beam from the transmission sample, was 0.00147 atom per barn thick, which corresponds to a thickness of 0.0266 centimeter and was maintained at room temperature throughout.

Thus, for each energy region and sample thickness there are six independent measurements: three temperatures in transmission, and three temperatures in self-indication.

Idaho Nuclear Corporation (INC) experiment - 1968. - A series of neutron transmission experiments designed to determine the variation in total cross section as a function of temperature at 2 keV were performed at the Idaho Nuclear Corporation's Materials Testing Reactor in 1968 (refs. 6 and 7). A scandium filter was used as a monochromator for 2-keV neutrons. The minimum value of scandium's total neutron cross section at 2 keV allows its use as an energy filter for neutrons. A 84-centimeter (33-in.) thick scandium filter was placed in the INC Materials Testing Reactor's fast chopper beam, and the transmitted neutron spectrum was measured. Part of the scandium-filtered spectrum is shown in figure 6.

The 2-keV beam should make it possible to observe the temperature dependence of neutron cross sections caused by the Doppler effect over the energy width of the beam. The resolution of the beam is broad enough to contain a sizeable number of resonances (~200 levels), thus providing a measure of average behavior.

The neutron transmission of a 0.508-centimeter (0.200-in.) thick tantalum sample

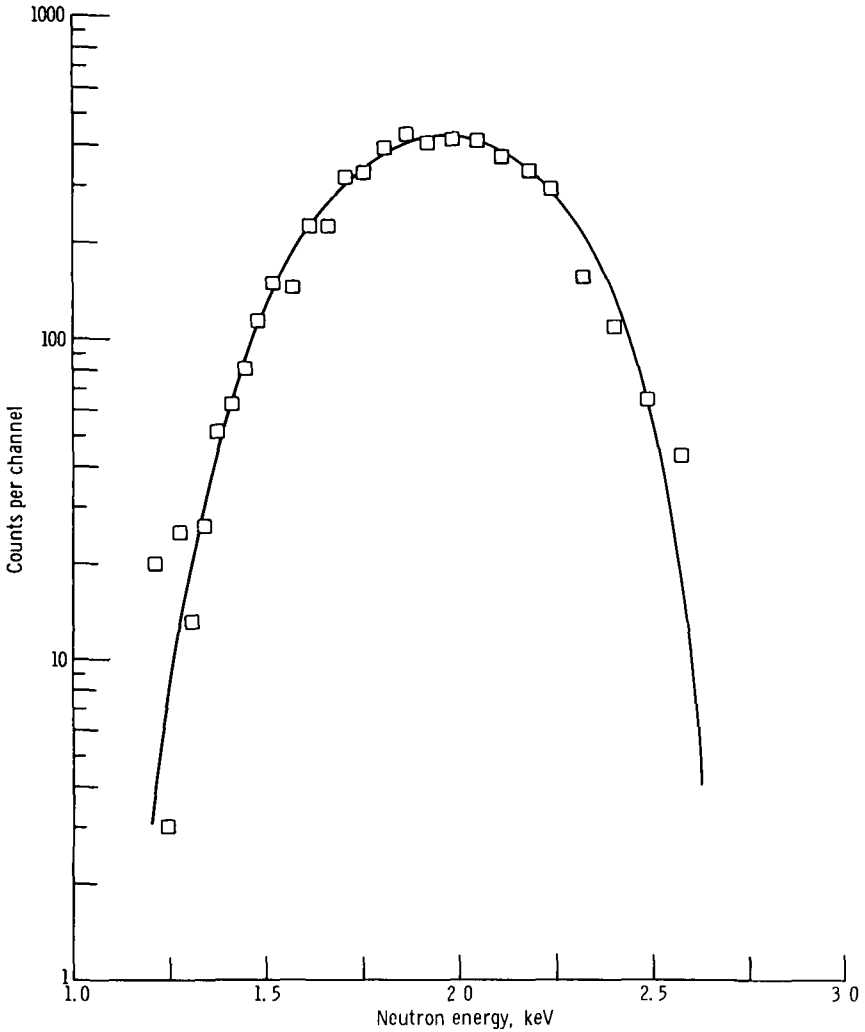

Figure 6 - Portion of scandium-filtered-beam spectrum of INC 1968 (refs 6 and 7) (Data from O. D. Simpson of Idaho Nuclear Corp , private communication) Solid line shown is hand drawn to guide the eye.

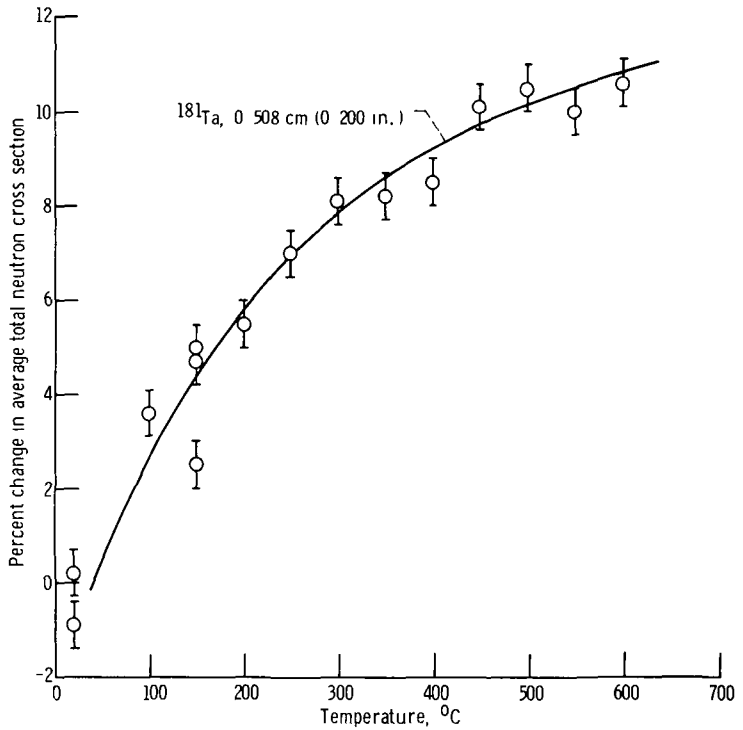

Figure 7 - Percentage charge in average neutron cross section as function of temperature is shown for three different samples. Error bars represent counting statistics only (Data from ref 7)

was measured as a function of temperature. The percentage increase in total cross section as a function of temperature as measured in the INC experiment is shown in figure 7.

COMPUTER SIMULATION OF RPI 1971 EXPERIMENTS

The results of the RPI 1971 experiments have been reduced to effective average total cross sections in the following manner: An effective average total cross section may be directly calculated from the average transmission $\overline{T}$ by

$$\overline{\sigma}_t = \left(\frac{-1}{nt}\right) \ln (\overline{T}) \tag{15}$$

where n is the number density of nuclei per cubic centimeter and t is the transmission sample thickness in centimeters. Another effective average total cross section may be defined from the average self-indication ratio $\overline{S}$ by the equation

$$\left(\overline{\sigma}_t\right)_s = \left(\frac{1}{nt}\right) \ln (\overline{S}) \tag{16}$$

where t is the thickness of the shielding sample in centimeters. It can be shown that the effective total cross sections are related to the true average total cross section $\overline{\sigma}$ by the inequality

$$\left(\overline{\sigma}_t\right)_s > \overline{\sigma} > \overline{\sigma}_t \tag{17}$$

see appendix B.

Given a set of DAISY-generated spin-dependent resonance parameters over the energy range of average cross sections, we may compute continuous cross sections by using a Doppler-broadening computer code (ref. 22). Since tantalum has a substantial Debye temperature (refs. 23 and 24), $\theta_D = 231$ K, we must use an effective temperature rather than the "true" thermodynamic temperature in the Doppler-broadening computation of the cross sections. The method of Lamb (refs. 25 and 26) has been used to generate the effective temperature. Tantalum is assumed to be a Debye solid. The following formula was solved by numerical quadrature for the effective temperature T^*:

$$T^* = \left(\frac{3}{2}\right) \theta_D \int_0^1 x^3 \coth\left(\frac{x\theta_D}{2T}\right) dx \tag{18}$$

TABLE IV. - EFFECTIVE TEMPERATURE T^*(K) OF TANTALUM AS FUNCTION OF THERMODYNAMIC TEMPERATURE T(K) FOR DEBYE TEMPERATURE OF 231 K

T	T^*	T	T^*
1	86.6	400	406 6
50	93 5	500	505 3
100	125.1	600	604.4
150	167.3	700	703.8
200	213.1	800	803.3
250	260.6	900	903.0
300	308.8	1000	1002.7

where T is the thermodynamic temperature. Table IV displays effective temperatures of tantalum for selected thermodynamic temperatures. It can be seen that reducing the thermodynamic temperature of tantalum below that of liquid nitrogen would not reduce the effective temperature of tantalum significantly. The effective temperatures used in the RPI 1971 computer simulations were 110.5, 300.1, and 1075.5 K, for the liquid-nitrogen-temperature, room-temperature, and high-temperature samples, respectively.

Two separate chains are generated for both s-wave J-states of tantalum. This procedure is followed to preclude the effect of merged cross-section sets (ref. 27). For these two separate chains, $\overline{\Gamma}_n^0(J = 3)$ is made equal to $\overline{\Gamma}_n^0(J = 4)$; and likewise with $\overline{D}(J = 3)$ and $\overline{D}(J = 4)$, which are set equal to 8.6 eV. Once these continuous cross sections have been calculated, we may use these cross sections in a computer simulation of the RPI 1971 experiments.

The average transmission of a 1/E neutron beam through a slab of material in an energy region from E_{low} to E_{high} may be computed by the following formula:

$$\overline{T} = \frac{\sum_{i=1}^{N} \left(\frac{1}{E_i}\right) \left\{\exp\left[-nt\sigma(E_i)\right]\right\}}{\sum_{i=1}^{N} \left(\frac{1}{E_i}\right)} \tag{19}$$

where $E_i = E_{low} + \left[i(E_{high} - E_{low})/N\right]$, $\sigma(E_i)$ is the value of σ_t (computed) at E_i and

N is the number of cross sections tabulated in the interval $\left[E_{low}, E_{high}\right]$. This expression, formula (19), is essentially exact for the RPI 1971 experiments, as any neutron that is scattered by the transmission sample is removed from the beam and not counted. The transmission so computed is transformed to a $\bar{\sigma}_t$ by equation (15) and can be compared directly with the measured $\bar{\sigma}_t$'s.

The average self-indication ratio $\bar{S}$ of a 1/E neutron beam through a slab of thickness t onto a thin self-indication sample of thickness t^* may be approximated by the formula

$$\bar{S} \doteq \frac{\sum_{i=1}^{N} \left(\frac{1}{E_i}\right) \exp\left[-n\sigma(E_i)t\right] \frac{\sigma_\gamma(E_i)}{\sigma_t(E_i)} \left\{1 - \exp\left[n\sigma_t(E_i)t^*\right]\right\}}{\sum_{i=1}^{N} \left(\frac{1}{E_i}\right) \frac{\sigma_\gamma(E_i)}{\sigma_t(E_i)} \left\{1 - \exp\left[n\sigma_t(E_i)t^*\right]\right\}} \tag{20}$$

where $\sigma_t(E_i)$ is the total cross section of the self-indication sample evaluated at E_i, $\sigma_\gamma(E_i)$ is the capture cross section of the self-indication sample evaluated at E_i, and all other symbols have the same meaning as in equation (19). Equation (20) does not include corrections for multiple scattering in the self-indication detector sample and is thus an approximate relation. The approximation involved in equation (20) has been checked by a single scattering model and by Monte Carlo simulation of multiple scattering in the detector sample. Equation (20) is found to be quite accurate, within 0.5 percent in calculating the self-indication ratio.

The value of $\bar{S}$ obtained from formula (20) may be converted into a $\left(\bar{\sigma}_t\right)_s$ by equation (16) and can be compared to the $\left(\bar{\sigma}_t\right)_s$'s resulting from measurements of $\bar{S}$. Recall from inequality (17) that these two values, $\bar{\sigma}_t$ computed from transmission and $\left(\bar{\sigma}_t\right)_s$ computed from the self-indication ratio, should bracket the true average total cross section.

Using formulas (19) and (20) and DAISY-generated resonance parameters, the RPI 1971 experiments may be accurately simulated on a computer.

Temperature-Dependent Analysis of RPI 1971 Experiment

In this section the analysis of the RPI 1971 temperature-dependent experiments at approximately 2 keV is detailed. Figure 5 illustrates the transmission data obtained in

the RPI 1971 experiments. The precision of the experimental results is such that structure caused by changes in the local strength function is readily discernible in the unresolved region. It is clear that if we wish to model the detailed cross-section behavior actually measured, we must attempt to extract the local strength functions and an analogous set of resonance parameters. The region about 2 keV has been chosen for this analysis as it appears to be a region of particularly high transmission and consequently low strength, thus providing a severe test of the technique. The 2-keV region has also been chosen since there exists other temperature-dependent neutron transmission data for tantalum at this energy (refs. 6 and 7).

Since the energy region chosen for pseudo-resonance analysis is rather narrow (192.0 eV at 4.3 eV per level, or 45 levels), we should not expect that the local average of Γ_n^0 over these 45 levels will be exactly $\overline{\Gamma}_n^0$. In fact, if we assume several values of $\overline{\Gamma}_n^0$ from the range allowed for the global average of Γ_n^0, the probability table (table V) indicates the probability levels of various results. For example, if the global value of $\overline{\Gamma}_n^0$ is 1.5 meV, the probability of a local average of Γ_n^0 for 45 levels less than 1.4 meV is 40 percent. As can be seen from the probability table, the range of

TABLE V. - PROBABILITY TABLE OF LOCAL AVERAGE REDUCED SCATTERING WIDTH $\overline{\Gamma}_n^0$ (local) FOR DIFFERENT VALUES OF AVERAGE REDUCED SCATTERING WIDTH $\overline{\Gamma}_n^0$

Probability of local average of 45 Γ_n^0's being greater than or equal to $\overline{\Gamma}_n^0$ (local)	$\overline{\Gamma}_n^0$ (local), meV, if $\overline{\Gamma}_n^0$ is -			
	1.0 meV	1.5 meV	2.0 meV	2.5 meV
0.001	0.471	0.706	0.941	1.177
.005	.539	.809	1.079	1.349
.010	.575	.863	1.150	1.438
.050	.680	1.020	1.360	1.701
.100	.741	1.112	1.482	1.853
.200	.820	1.230	1.640	2.050
.300	.880	1.320	1.760	2.200
.400	.933	1.400	1.867	2.333
.500	.985	1.478	1.970	2.463
.600	1.039	1.559	2.078	2.598
.700	1.099	1.648	2.198	2.747
.800	1.172	1.757	2.343	2.929
.900	1.278	1.917	2.555	3.194
.950	1.370	2.055	2.740	3.425
.990	1.555	2.332	3.110	3.888
.995	1.627	2.440	3.253	4.067
.999	1.781	2.672	3.563	4.453

$\overline{\Gamma}_n^0$ (local) is rather large even for a region containing 45 levels. Thus, a method has been adopted in this study which will determine the local value of $\overline{\Gamma}_n^0$. This is done by seeking regions wherein $\overline{\Gamma}_n^0$ (local) and σ_{pot} provide temperature-dependent effective total cross sections which are compatible with the RPI 1971 experimental results and minimize the difference between the local average and the measured averages.

The computer simulation can compute quantities similar to those measured, that is, the average transmission and the average self-indication ratio. We can present the simulation results, as well as the measurements in terms of average effective total cross sections, by the use of equations (15) and (16). The average effective total cross sections generated by the computer simulation can be represented as a resonance-cross-section contribution plus the potential cross section. Several values of $\overline{\Gamma}_n^0$ (local) have been used in these computer simulations. The results of these simulations are shown in tables VI and VII. If we compare the nominal values shown in tables VI and VII with the measured values of table III, we realize that the use of global averages in this region predicts a Doppler effect of more than double that observed and a total cross section about 30 percent larger than that observed. Thus, it is clear that, to adequately model the cross-section behavior, local values must be used.

Subtracting the potential contribution from the average effective total cross section leaves what will be called the resonance contribution to the average effective total cross section. This resonance contribution to the total cross section has been spline interpolated and plotted as a function of the local value of $\overline{\Gamma}_n^0$ for the three temperatures: cold, room, and high. In figures 8 and 9 the resonance portions of the average effective

TABLE VI. - AVERAGE VALUES OF LOCAL PSEUDO-RESONANCE PARAMETERS AND RESULTANT EFFECTIVE TOTAL CROSS SECTIONS COMPUTED FOR 0 5-CENTIMETER-THICK TANTALUM SLAB

	Nominal	Variations from nominal case						
		1	2	3	4	5	6	7
Potential cross section, σ_{pot}, barns	8.5	8.5	8 5	8.5	9 0	9.0	9.0	9.5
Average reduced scattering width, $\overline{\Gamma}_n^0$, eV	002	.0015	.001	.00086	.00086	.00086	0005	.0007
Average capture width, $\overline{\Gamma}_\gamma$, eV	.052	.052	.052	.052	052	.045	.052	.052
Effective average total cross section, $\overline{\sigma}_t$, barns, at -								
77 K	18.50	16.75	14.80	14.19	14.69	14.69	12.88	14.42
295 K	20 41	18.31	15.89	15.12	15 12	15.61	13.37	15.17
1073 K	23.37	20.51	17.25	16.24	16.75	16.75	13.88	16.01
Effective average total cross section defined from average self-indication ratio, $(\overline{\sigma}_t)_s$, barns, at -								
77 K	44.57	40.28	34.77	32.85	33.34	33.15	27.05	31.29
295 K	47.97	42.64	35.83	33.51	34.00	33.70	26.68	31.51
1073 K	45.79	39.63	32.22	29.83	30 36	30.10	23.23	27.85

TABLE VII. - AVERAGE VALUES OF LOCAL PSEUDO-RESONANCE PARAMETERS AND RESULTANT EFFECTIVE TOTAL CROSS SECTIONS COMPUTED FOR 1 0-CENTIMETER-THICK TANTALUM SLAB

	Nominal	Variations from nominal case						
		1	2	3	4	5	6	7
Potential cross section, σ_{pot}, barns	8 5	8.5	8 5	8.5	9.0	9 0	9.0	9.5
Average reduced scattering width, $\overline{\Gamma}_n^0$, eV	002	.0015	001	00086	.00086	.00086	0005	.0007
Average capture width, $\overline{\Gamma}_\gamma$, eV	.052	052	.052	052	.052	045	052	.052
Effective average total cross section, $\overline{\sigma}_t$, barns, at -								
77 K	15.35	14.30	13.10	12 72	13 21	13.21	12.05	13.22
295 K	16.98	15 71	14 19	13 69	14.19	14.17	12.64	14.04
1073 K	19.94	18.06	15.80	15.06	15.58	15.57	13.36	15.13
Effective average total cross section defined from average self-indication ratio, $(\overline{\sigma}_t)_S$, barns, at -								
77 K	33.89	31.33	27.98	26 80	27.27	27 16	23.29	26 16
295 K	38.25	34.96	30 48	28.89	29 37	29.14	24.11	27.74
1073 K	38 94	34.65	29.12	27.26	27.80	27.57	22.00	25.88

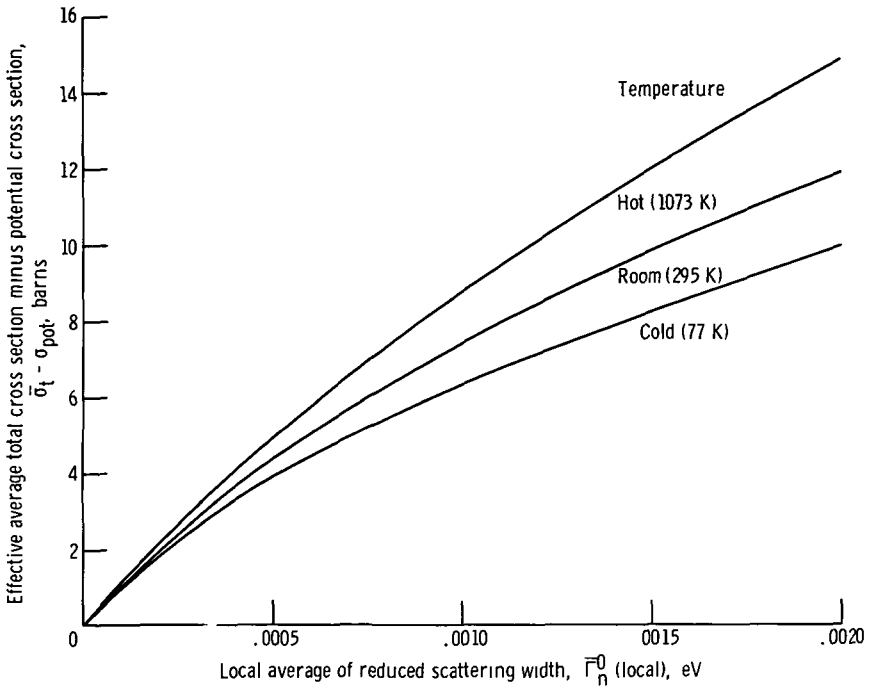

Figure 8. - Resonance portion of effective total cross section as determined from transmission through 0.5-centimeter-thick slab of tantalum as function of local value of average reduced scattering width between 1825 0 and 2017.0 eV. Average level spacing, 4.3 eV; average capture width, 0.052 eV.

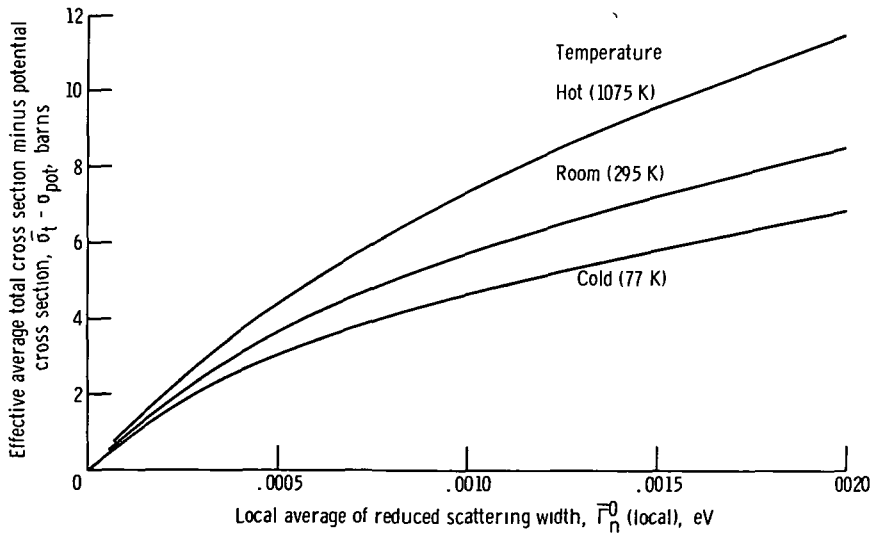

Figure 9. - Resonance portion of effective total cross section as determined from transmission through 1 0-centimeter-thick slab of tantalum as function of local value of average reduced scattering width between 1825.0 and 2017.0 eV. Average level spacing, 4.3 eV; average capture width, 0.052 eV.

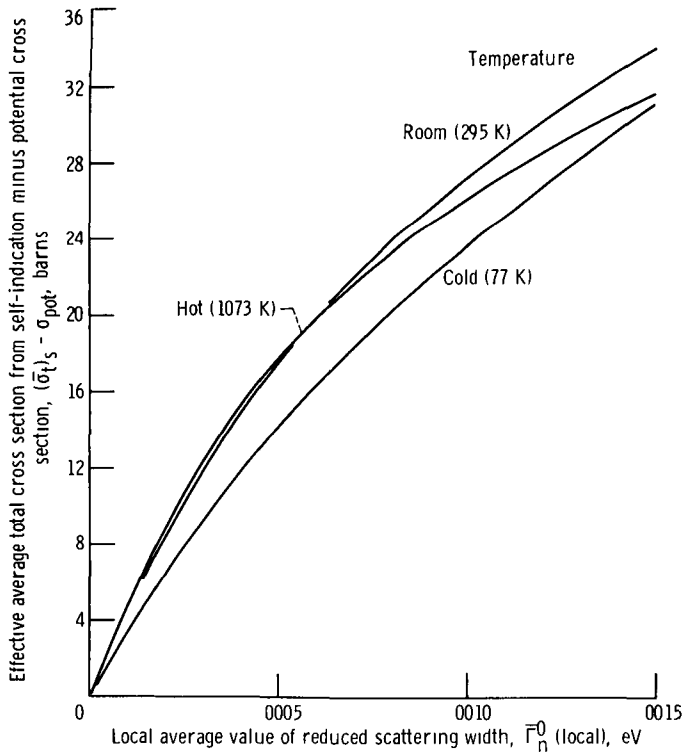

Figure 10 - Resonance portion of effective total cross section as determined from self-indication through 0 5-centimeter-thick slab of tantalum as function of local value of average reduced scattering width between 1825 0 and 2017 0 eV Average level spacing, 4 3 eV, average capture width, 0 052 eV; thickness of self-indication sample, 0 0266 centimeter; temperature of self-indication sample, 295 K throughout experiment

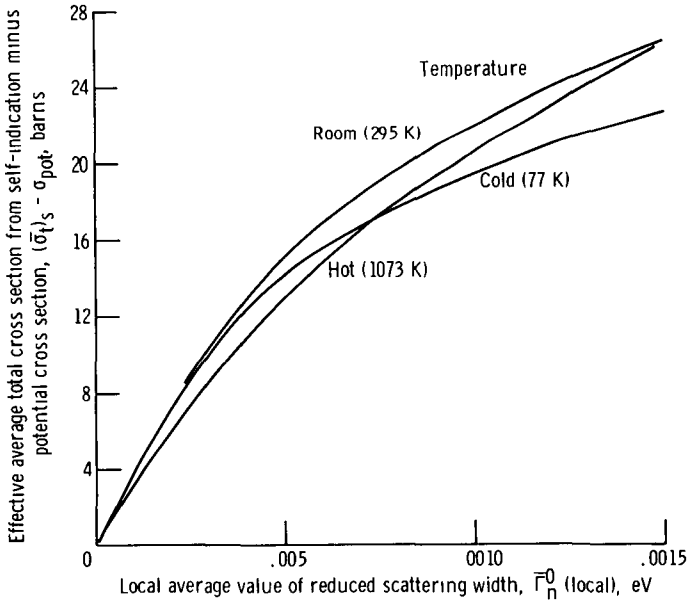

Figure 11 - Resonance portion of effective total cross section as determined from self-indication through 1.0-centimeter-thick slab of tantalum as function of local value of average reduced scattering width between 1825 0 and 2017.0 eV. Average level spacing, 4 3 eV; average capture width, 0 052 eV; thickness of self-indication sample, 0.0266 centimeter, temperature of self-indication sample, 295 K throughout experiment

total cross section determined by transmission have been plotted as a function of $\overline{\Gamma}_n^0$ (local). In figures 10 and 11 the resonance portions of the average effective total cross section determined by self-indication have been plotted as a function of $\overline{\Gamma}_n^0$ (local). It should be noted that the change of average effective total cross section with respect to a change in local strength is nonlinear. The smooth curves shown in the figures are spline approximations (ref. 28) obtained by using Akima's approximation (ref. 29) for the end-point slopes.

In the same way, the measured average effective total cross sections are also made up of a resonance portion and a potential cross section. Given these experimentally determined average effective total cross sections, we may subtract varying amounts of potential cross section and plot the remaining resonance portion and its error along the calculated resonance-cross-section curves of figures 8 to 11. For example, figure 12 shows the average effective resonance portion of the total cross section as determined by transmission for the 0.5-centimeter slab of tantalum at room temperature as a function of $\overline{\Gamma}_n^0$ (local). The experimentally measured value of the average effective total cross section, for the 0.5-centimeter room-temperature sample in transmission, is 15.67±0.83 barns. For a potential cross section of 8.5 barns the remaining 7.17±0.83 barns may be plotted on the curve. The limits of the rectangular region of figure 12 indicate the region of local $\overline{\Gamma}_n^0$'s which are compatible with a potential cross section of 8.5 barns and a $\overline{\sigma}_t$ measured by transmission through a 0.5-centimeter slab of tantalum at room temperature of 15.67±0.83 barns. The same process is repeated for all temperature measurements. If a region of consistent local $\overline{\Gamma}_n^0$'s is found with

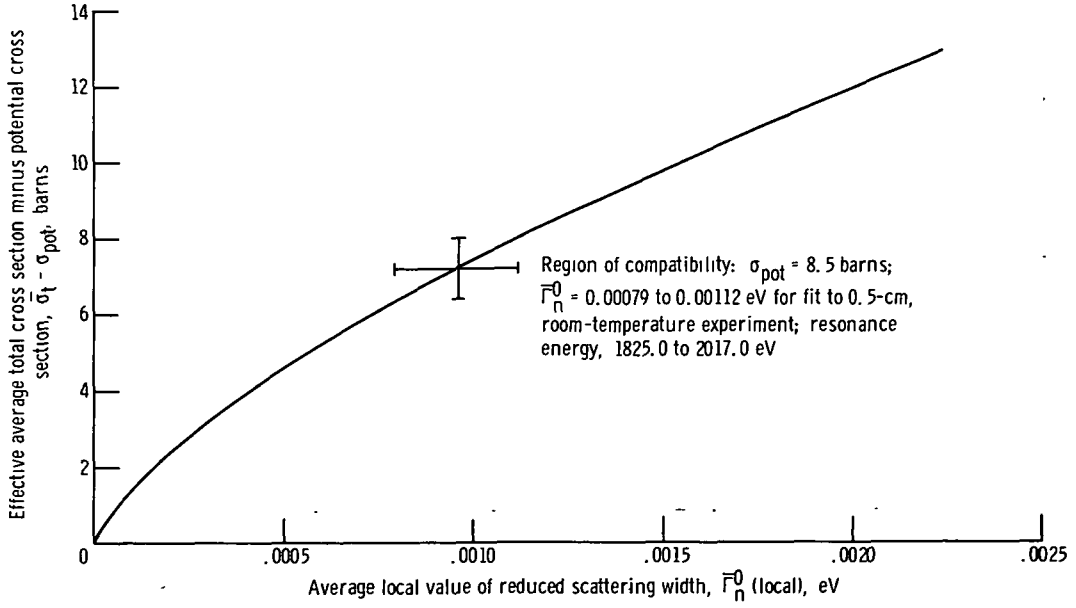

Figure 12. - Region of compatibility for 0.5-centimeter-thick slab of tantalum at room temperature and potential cross section of 8.5 barns.

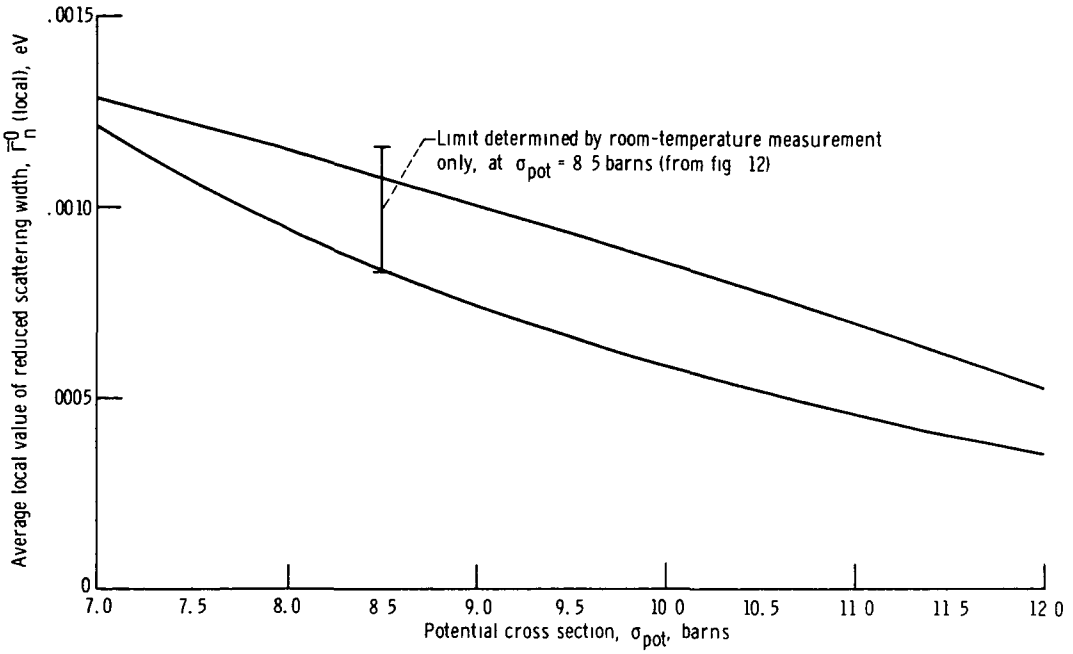

Figure 13 - Transmission-compatible region for 0 5-centimeter-thick tantalum slab Region enclosed by curves will produce resonance cross sections which are compatible with RPI 1971 experiments on 0 5-centimeter slab between 1825.0 and 2017 0 eV.

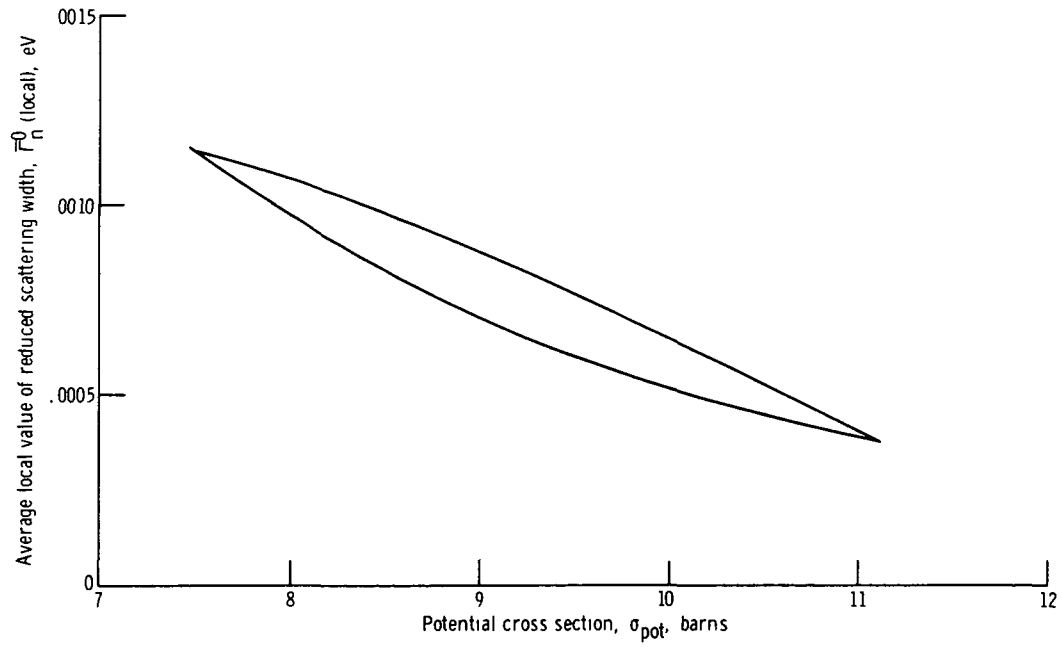

Figure 14. - Transmission-compatible region for 1.0-centimeter-thick tantalum slab Region enclosed by curves will produce resonance cross sections which are compatible with RPI 1971 experiments on 1 0-centimeter slab between 1825 0 and 2017 0 eV.

respect to all temperature measurements of a sample and a potential cross section, this region may be plotted on a potential-cross-section and $\overline{\Gamma}_n^0$ (local) chart, see figures 13 to 16. These provide us with areas in which the pseudo-resonance parameters chosen by DAISY match the experimental results of the RPI 1971 experiment.

It was found (cf. figs. 13 to 16) that the thick (1.0 cm) sample of tantalum in transmission provided the most stringent region of compatible parameters. The thin (0.5 cm) sample of tantalum in self-indication showed no region of compatibility with reasonable variations of the resonance parameters. However, it should be recognized that the self-indication regions of compatibility did not appear to be particularly sensitive to changes of the local average resonance parameters. The regions of compatibility for self-

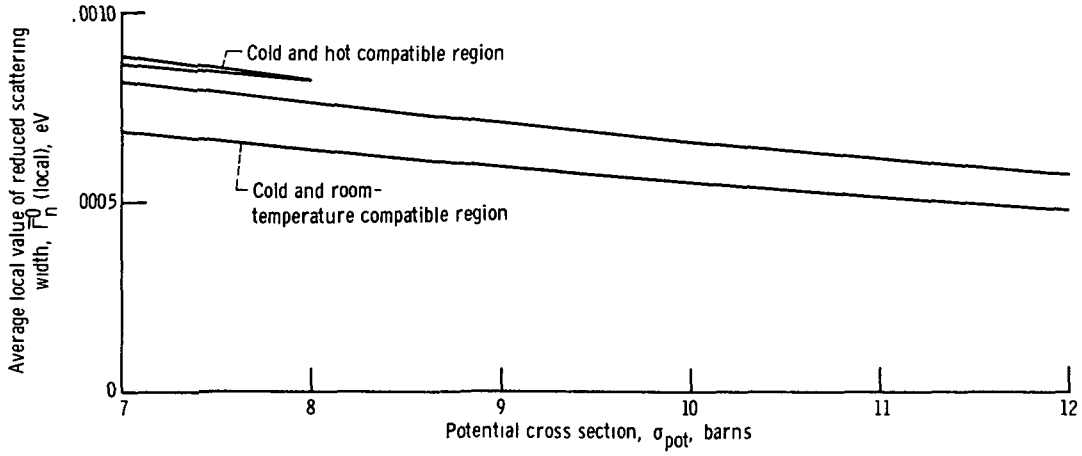

Figure 15. - Self-indication partially compatible regions for 0.5-centimeter-thick tantalum slab Regions enclosed by curves will produce resonance cross sections which are compatible, as labeled, with RPI 1971 experiments on 0.5-centimeter slab between 1825.0 and 2017.0 eV.

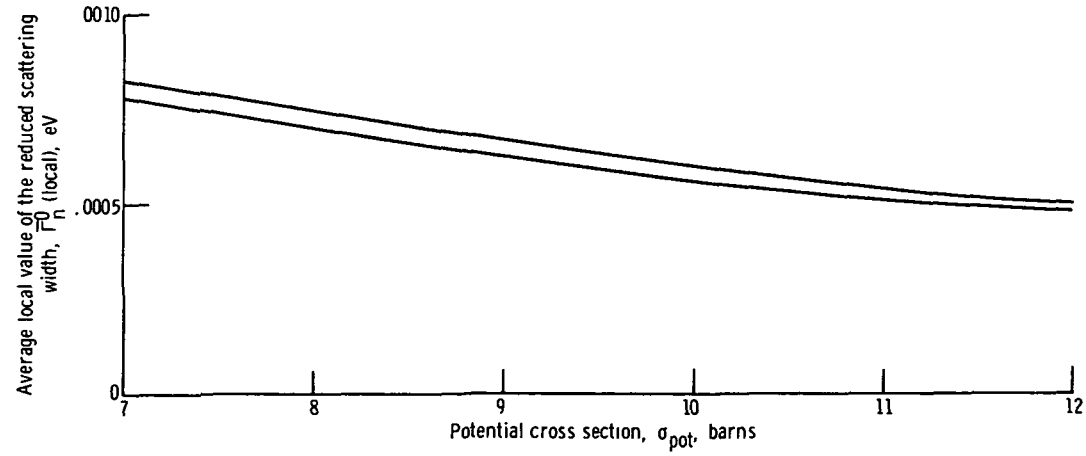

Figure 16. - Self-indication compatible region for 1.0-centimeter-thick tantalum slab. Region enclosed by curves will produce resonance cross sections which are compatible with RPI 1971 experiments on 1.0-centimeter slab between 1825.0 and 2017.0 eV.

indication experiments are bands which are nearly horizontal. The regions of compatibility for the transmission experiments are lunes of relatively small area. Thus, the transmission data have been given more weight in the choice of final compatible parameters than the self-indication data.

It may be seen from observation of figure 5 that the behavior of tantalum's cross section is not smooth even with the 10 percent energy bins chosen. Also at 2 keV the local strength must be rather low as the transmission is enhanced. This is in agreement with the findings of this report and is caused by the local clustering or sparsity of resonances and/or the local strength of the resonances in these energy bins. Since there appear to be significant differences in the local strength functions, the present analysis demonstrates a technique for the extraction of the local strength function from temperature-dependent transmission and self-indication measurements. The technique demonstrated may be used to provide sets of pseudo-resonances whose individual parameters obey the appropriate statistical distributions and whose average behavior simulates the transmission and self-indication measurements within experimental error.

Tables VI and VII give the average values of the local pseudo-resonance parameters and the results of the computer simulations which use cross sections generated from these parameters. These tables allow us to ascertain the sensitivity of the effective total cross sections to changes in the pseudo-resonance parameters. It can be clearly seen from a comparison of variations 3 and 4 of the tables that, at least in this range of average parametric values, the changes in the effective total cross sections are directly proportional to the changes in the potential cross section. That is, a change of +0.50 barn in the potential cross section produces almost a uniform increase of 0.50 barn in the effective total cross sections inferred from transmission and self-indication simulations.

It may be observed by the comparison of variations 4 and 5 that the change in the average value of $\overline{\Gamma}_\gamma$ from 0.052 eV to 0.045 eV leaves the average effective total cross section inferred from transmission virtually unchanged. This change does alter the value of the average effective total cross section inferred from self-indication. This is caused by the changes produced in the capture cross section. The changes produced by altering $\overline{\Gamma}_\gamma$ are of second order compared to the changes produced by the local strength and the potential cross section. We can thus "fine tune" the final cross-section set by altering the average value of the capture width.

As the self-indication experiments were subject to larger errors than the transmission experiments, the values of σ_{pot} (consistent) and $\overline{\Gamma}_n^0$ (local consistent) were chosen to fit all transmission experiments and to fit most of the self-indication experiments. The values chosen to fit the RPI 1971 experiment in the energy region from 1825.0 to 2017.0 eV were σ_{pot} = 9.5 barns and $\overline{\Gamma}_n^0$ (local) = 7.0×10^{-4} eV. These values, along with a $\overline{\Gamma}_\gamma$ of 52 meV, fitted within the error bars of all transmission experiments and four out of six self-indication experiments, figures 17 and 18. The result of a recent

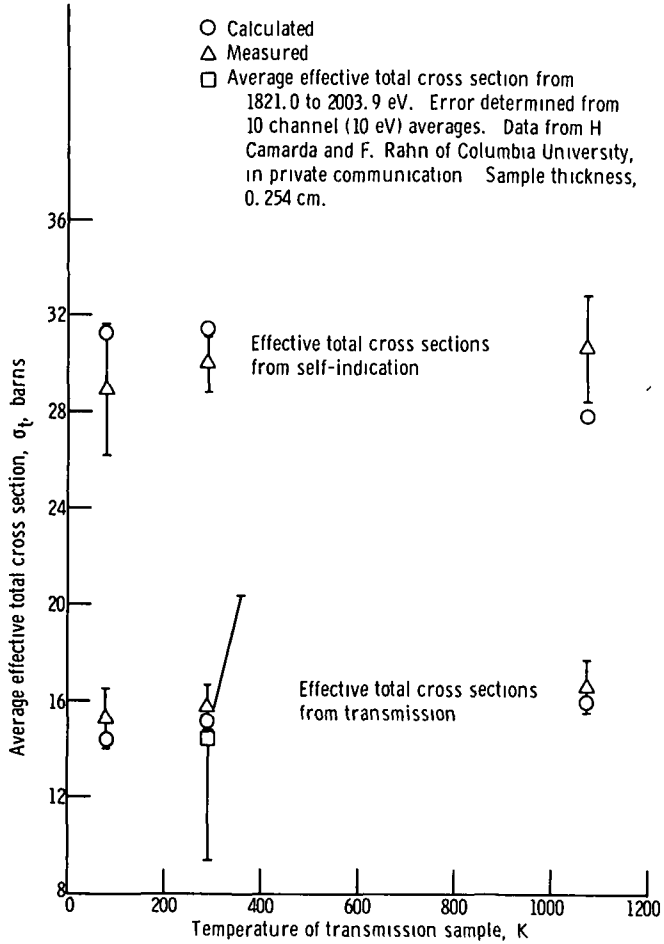

Figure 17 - Comparison of measured and calculated average effective total cross sections, from transmission and self-indication ratio experiments, as function of temperature for 0.5-centimeter-thick tantalum slab.

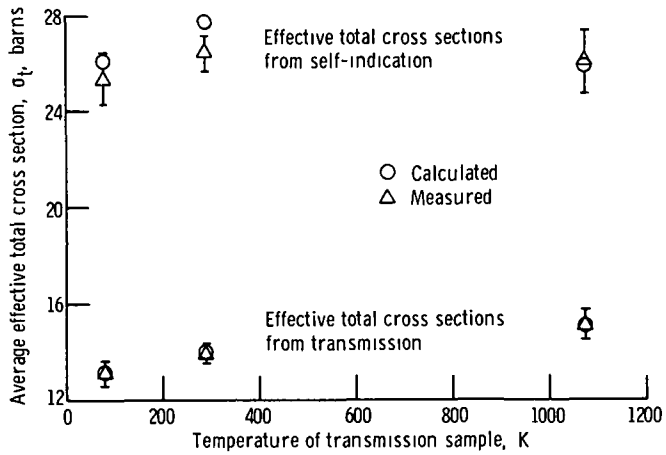

Figure 18. - Comparison of measured and calculated average effective total cross sections, from transmission and self-indication experiments, as function of temperature for 1.0-centimeter-thick tantalum slab.

high-resolution transmission experiment is also shown in figure 17 (private communication of 1968 data from F. J. Rahn and H. Camarda of Columbia University).

A list of the DAISY-generated compatible resonance parameters for the energy region 1825.0 to 2017.0 eV is shown in table VIII. This table is then the final result of the analysis of the RPI 1971 experiment. These parameters, while not unique, will adequately model the temperature-dependent behavior of tantalum at 2 keV and are suitable for use in unresolved resonance reactor calculations.

TABLE VIII - RESONANCE PARAMETERS USED FOR COMPUTED CROSS SECTIONS SHOWN IN FIGURES 17 AND 18

[Seventh variation used in RPI 1971 experiment (ref. 5), average reduced scattering width, $\overline{\Gamma}_n^0$, 0 70 meV, capture width, Γ_γ, 52 meV; potential cross section, σ_{pot}, 9.5 barns]

(a) Average level spacing, D(J = 4), 8 6 eV, statistical factor, g, 0.5625

Resonance energy, E, eV	Scattering width, Γ_n, eV
1825 0000	0.02990399
1825 3337	01448790
1833 4493	00087920
1841.6215	.04647899
1851.3175	00289850
1866.7056	.09095930
1877.8835	.17080720
1890.8943	.01664480
1900.0273	.07454510
1905.3980	.01845030
1912 4215	.00064009
1916 0287	.00000240
1928.3157	00040600
1944.2893	.00453179
1949 8231	.00001340
1954.1996	00867499
1962 6062	00687890
1967 5294	04249540
1977.7147	.00701980
1992.3089	.07792800
2009.2010	.05289979
2015 6339	.02148139
2019 5734	03189699
2022 6075	.01492579

(b) Average level spacing, D(J = 3), 8 6 eV, statistical factor, g, 0.4375

Resonance energy, E, eV	Scattering width, Γ_n, eV
1825.0000	0 02990399
1832.6116	.01888040
1838 6334	05318150
1850.6213	.00016689
1860.2224	01661870
1875.3686	.02331850
1892 0088	02956620
1900.6927	10772499
1903 4424	.00773039
1916 9520	.05056860
1922.2507	.06293280
1942.2597	.00004520
1946.6656	.15881540
1955.8728	.01033830
1959 7644	06480910
1964.1843	.00071040
1965.1088	.04471409
1971 5433	.03200819
1982.1331	.00262450
1989.3610	.00197519
1997.3739	.00122420
2011.6603	.00064850
2016.4285	.00745690
2022 6306	.00777750

Temperature-Dependent Analysis of INC 1968 Experiment

In reference 7 an attempt was made to fit the temperature-dependent change in the total effective cross section of tantalum at approximately 2 keV by a pseudo-resonance technique. The change in the total cross section as a function of temperature for several pseudo-resonance chains and for the experimental data is shown in figure 19. It was concluded in reference 7 that the pseudo-resonance curves computed, labeled A, B, C, D, and F, did not adequately describe the experimental data. Why the pseudo-resonance approach failed in this test poses a serious problem.

Recall that the INC sample was 0.508 centimeter (0.200 in.) thick; this allows us to compare the INC experiment directly with the RPI 0.500-centimeter-thick sample. Since the scandium-filtered beam is considerably wider than the RPI energy resolution, the scandium beam shown in figure 6 has been broken into nine energy groups and folded over the RPI transmission data of figure 5. Two energy-averaged total effective cross sections were obtained over the scandium-filtered beam, one for room-temperature $\overline{\sigma}_t$ = 18.272 barns and one for the high-temperature (800° C) $\overline{\sigma}_t$ = 19.662 barns. Thus, the measured scandium-filtered beam folded over the RPI-measured effective cross sections gave a ratio of hot to room-temperature total cross sections of 1.076 at 800° C.

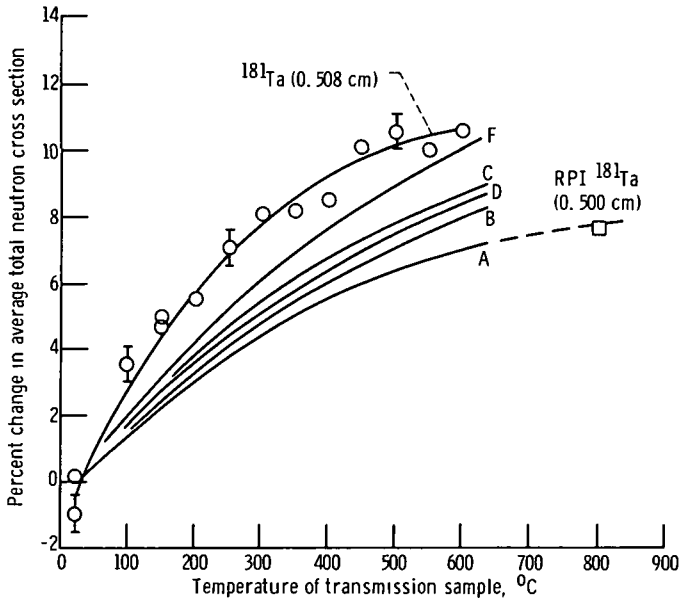

Figure 19. - Percentage change in average effective total cross section as function of temperature. Scandium-filtered beam of 2-keV neutrons; average level spacing, 4.3; ratio of average reduced scattering width to average level spacing, 1.8×10^{-4}. Curves A, B, C, D, and F represent five different sets of mock data that have been Doppler broadened as a function of temperature. Point labeled RPI ^{181}Ta represents the RPI effective cross sections folded over the scandium-filtered spectrum. (Data from ref. 7.)

This point has been plotted on figure 19. It is seen that this point is in good agreement with the "A-set" of pseudo cross sections generated in reference 7. Such agreement suggests that perhaps the experimental values of INC 1968 are subject to some source of experimental bias toward larger changes in the average effective cross section with respect to changes in temperature. This was, in fact, the case as the collimator into which the scandium was inserted had an intolerable amount of leakage through duct streaming (ref. 30). Thus, the tantalum sample was not only exposed to a 2-keV beam but also to a reactor-like beam of duct streaming neutrons which would serve to accentuate the Doppler effect measured. This deficiency has been noted and the scandium-filter - collimator system has been redesigned (ref. 31). However, the experiment has not been conducted with the new 107-centimeter (42-in.) scandium-filter - collimator system.

CONCLUSIONS

A temperature-dependent pseudo-resonance parameter analysis has been performed on tantalum at 2-keV neutron energy. An earlier temperature-dependent analysis in this energy region has been discussed. The following conclusions were drawn:

1. In portions of the unresolved neutron resonance region, where experimental resolution is adequate to encompass few resonances (<100) in a measurement the data permits the evaluation of the local strength function. Therefore, the local behavior of the measured neutron cross section may be modeled by the use of appropriately chosen pseudo-resonance parameters. These parameters may then be used in reactor calculations with a measure of credibility similar to that for resolved resonance parameters. The customary approach of using pseudo-resonance parameters based on an average strength function rather than a local strength function can be erroneous.

2. In the energy region 1825.0 to 2017.0 eV the temperature-dependent behavior of tantalum's effective total neutron cross section as determined by transmission has been adequately modeled by a specific set of pseudo-resonance parameters, using the technique described.

3. The technique illustrated in this report should be generally applicable to measurements in the unresolved neutron resonance region, provided that the inelastic and p-wave cross sections are either negligible or known. This technique provides a level of confidence that locally generated resonance parameters can model observed unresolved-cross-section behavior better than the naive sampling from global distributions.

4. The results of this study suggest that a Doppler coefficient calculated by sampling from grand average statistical distributions over the entire unresolved region can be in error since local variations in the strength function are not taken into consideration.

Lewis Research Center,
National Aeronautics and Space Administration,
Cleveland, Ohio, January 9, 1973,
503-25.

APPENDIX A

COMPUTER PROGRAM MOBEE

Over 300 resonance energies have been measured for tantalum. To compare the theoretical level spacing distribution with the distribution of the experimentally determined values, we could plot the cumulative distribution of all 305 level spacings and compare it to the theoretical level spacing for two uncorrelated spin species. However, we would find that the agreement is better with the single-species Wigner level spacing distribution than with the two-species distribution (figs. 1 and 20). This indicates that if the Wigner model applies, some closely spaced resonances have not been resolved in the region between 0 and 1397.9 eV. We could laboriously plot the cumulative distribution for selected energy intervals and attempt to find the region in which serious deviation between the theoretical distribution and the experimental distribution arises. A somewhat different approach has been adopted in the MOBEE computer code. It produces a plot of the experimental cumulative level spacing distribution and the theoretical cumulative level spacing distribution for each new experimentally measured level spacing in a 35-millimeter motion-picture format.

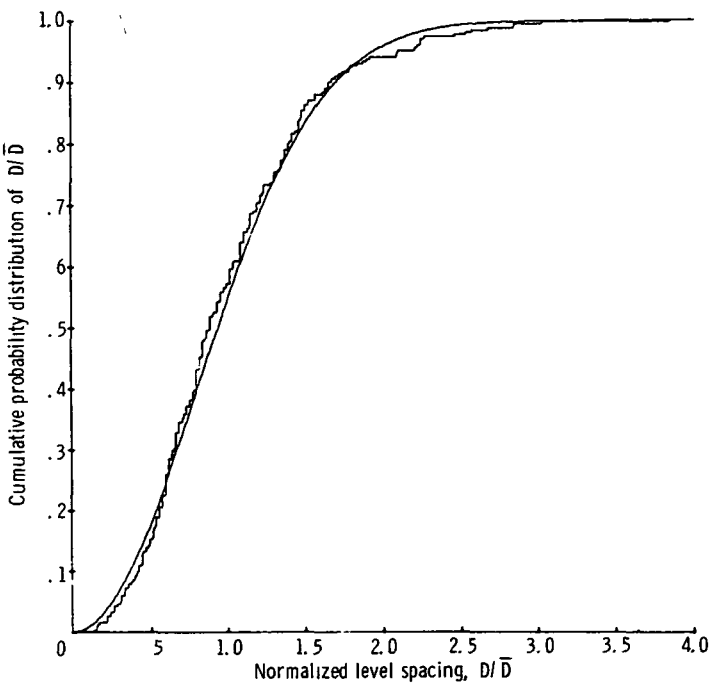

Figure 20. - Cumulative probability distribution of normalized level spacing compared to Wigner level spacing distribution for a single spin species - for first 300 level spacings reported in reference 17. Number of level spacings, 300; average level spacing of first 300 level spacings, 4.526 eV; energy E_0 of last resonance used in average and display, 1362.2 eV.

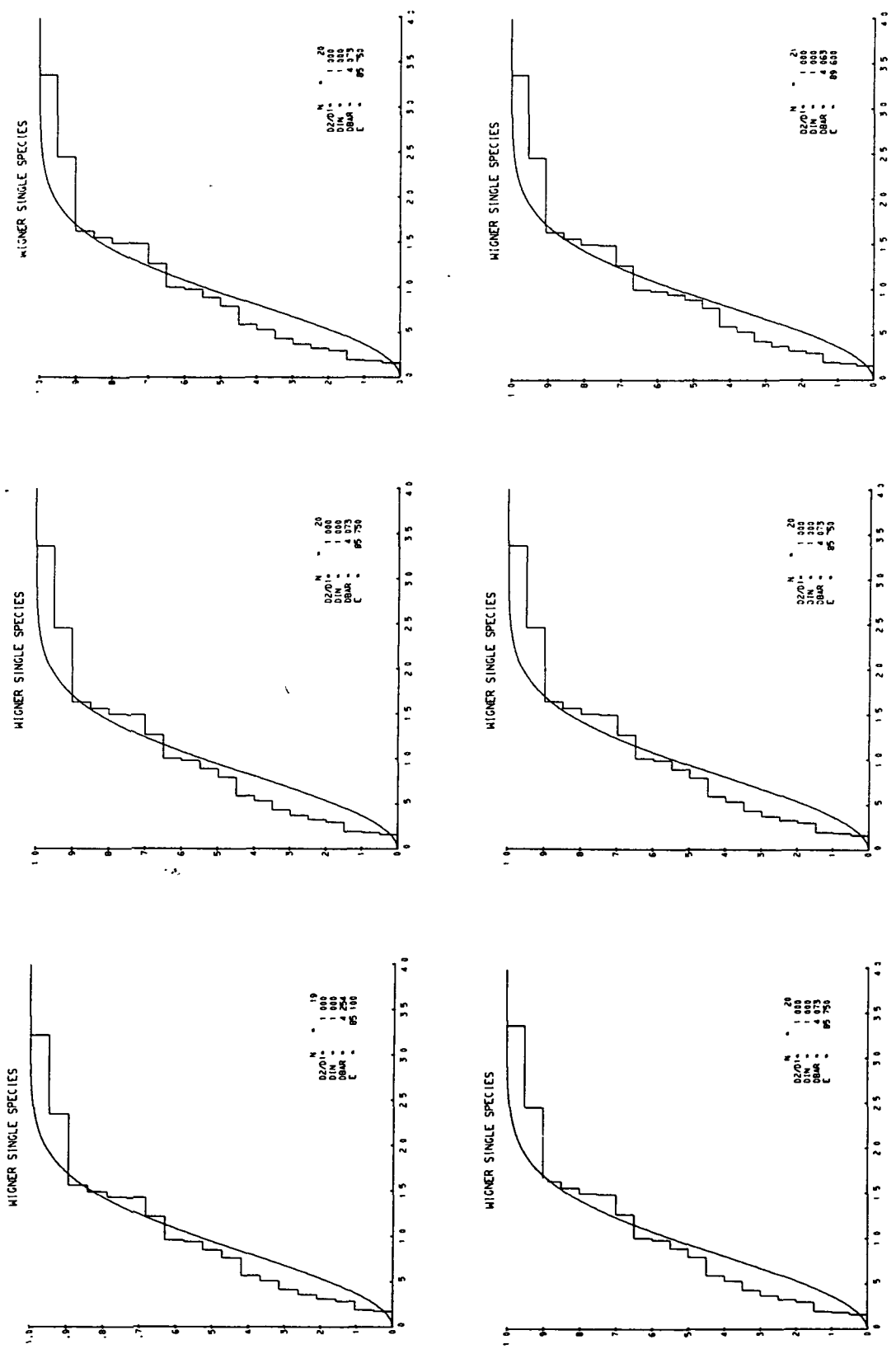

Figure 21. - Few representative frames (in order) of output from computer code MOBEE.

MOBEE, by the use of computerized microfilm plotting (ref. 32), produces a 35-millimeter motion picture of the experimental distribution's behavior relative to the theoretical distribution. By the use of a film editor, the viewer can easily see the point at which the experimental distribution begins to deviate significantly from the theoretical distribution. Sufficient fiducial data is listed on the film frame such that the $\overline{D}$ can be easily determined at that point.

A series of resonance cards, containing at least the value of E_0 for a resonance, are read in ascending order by MOBEE. At this point, several options are available to the code's user. He may specify an average level spacing $\overline{D}$ and let all distributions be plotted with this value as the mean value, or he may allow the code to compute averages. The experimental cumulative distribution of level spacings can be displayed with no theoretical distribution, with a theoretical single-species cumulative distribution, or with a theoretical double-species cumulative distribution shown. If the user chooses the double-spin-species option, he must supply the ratio of D_2/D_1, of the two spin states.

For illustrative purposes, a few frames from the MOBEE output are shown in figure 21.

The MOBEE code has been extremely useful in allowing the determination of the energy region in which closely spaced levels begin to be missed or not resolved.

APPENDIX B

COMPARISON OF AVERAGE EFFECTIVE TOTAL CROSS SECTIONS FROM TRANSMISSION AND SELF-INDICATION WITH AVERAGE TOTAL CROSS SECTION

The RPI 1971 experiments measured the average effective total cross section both from transmission and from self-indication. This appendix will indicate the relation of these quantities to the "true" average total cross section. This derivation follows that of Block and Byoun (ref. 32).

Since the transmission sample is located in a neutron beam, the average transmission $\langle T \rangle$ in the energy interval E_1 to E_2 is

$$\langle T \rangle = \frac{\int_{E_1}^{E_2} e^{-n_1 t \sigma(E)} \, dE}{\int_{E_1}^{E_2} dE} \tag{B1}$$

where n_1 is the number of nuclei per cubic centimeter in the transmission sample, t is the thickness of the transmission sample in centimeters, and $\sigma(E)$ is the total cross section as a function of energy. This may be rewritten as

$$\langle T \rangle = \frac{\int_{E_1}^{E_2} e^{-n_1 t[\sigma(E)+\langle \sigma \rangle - \langle \sigma \rangle]} \, dE}{E_2 - E_1} \tag{B2}$$

where $\langle \sigma \rangle$ is the "true" average total cross section between energies E_1 and E_2. By rearranging expression (B2) we have

$$\langle T \rangle = e^{-n_1 t \langle \sigma \rangle} \frac{\int_{E_1}^{E_2} e^{-n_1 t[\sigma(E)-\langle \sigma \rangle]} \, dE}{E_2 - E_1} \tag{B3}$$

or if we use brackets to again denote an energy average between energies E_1 and E_2,

$$\langle T \rangle = e^{-n_1 t \langle \sigma \rangle} \left\langle e^{-n_1 t [\sigma(E) - \langle \sigma \rangle]} \right\rangle \tag{B4}$$

We may then define

$$\eta \equiv \left\langle e^{-n_1 t [\sigma(E) - \langle \sigma \rangle]} \right\rangle \tag{B5}$$

as a cross-section fluctuation correction. If

$$\sigma(E) - \langle \sigma \rangle < \frac{1}{(n_1 t)} \tag{B6}$$

then we may approximate η.

$$\eta = \left\langle e^{-n_1 t [\sigma(E) - \langle \sigma \rangle]} \right\rangle \doteq 1 + \frac{1}{2} n_1^2 t^2 \, \mathrm{var}[\sigma(E)] \tag{B7}$$

since $\mathrm{var}[\sigma(E)] = \langle \sigma^2(E) \rangle - \langle \sigma \rangle^2$. As the effective average total cross section is calculated directly from the average transmission, we have

$$\langle \sigma_t \rangle = \left(\frac{-1}{n_1 t} \right) \ln \langle T \rangle \tag{B8}$$

for the average effective total cross section from transmission, or

$$\langle \sigma_t \rangle = \langle \sigma \rangle - \frac{1}{n_1 t} \ln \eta \tag{B9}$$

From approximation (B7), we find $\eta \geq 1$; thus,

$$\langle \sigma_t \rangle < \langle \sigma \rangle \tag{B10}$$

Here then we have shown the relation of the average effective total cross section as determined by transmission $\langle \sigma_t \rangle$ and the average total cross section $\langle \sigma \rangle$.

The average self-indication ratio $\overline{S}$ may be defined as follows:

$$\overline{S} = \frac{\left\langle Y_\gamma(E) e^{-n_1 t \sigma(E)} \right\rangle}{\langle Y_\gamma(E) \rangle} \tag{B11}$$

where $Y_\gamma(E)$ is the capture yield at energy E for the self-indication capture sample. The capture sample has n_2 nuclei per cubic centimeter and is t_2 centimeters thick. Neglecting multiple scattering effects within the thin capture sample ($n_2 t_2$ is only 0.00147/barn) the capture yield may be approximated by

$$Y_\gamma(E) \doteq \frac{\sigma_\gamma(E)}{\sigma(E)} \left[1 - e^{-n_2 t_2 \sigma(E)} \right] \tag{B12}$$

where $\sigma_\gamma(E)$ is the capture cross section at energy E. Since $n_2 t_2 \sigma(E)$ is small in the unresolved region, we can expand the exponential and approximate

$$1 - e^{-n_2 t_2 \sigma(E)} \doteq n_2 t_2 \sigma(E) \tag{B13}$$

Hence,

$$Y_\gamma(E) \doteq \frac{\sigma_\gamma(E)}{\sigma(E)} n_2 t_2 \sigma(E)$$

$$\doteq n_2 t_2 \sigma_\gamma(E) \tag{B14}$$

Combining equations (B12) and (B14) yields the following approximation for the self-indication ratio:

$$\bar{S} \doteq \frac{\left\langle n_2 t_2 \sigma_\gamma(E) e^{-n_1 t \sigma(E)} \right\rangle}{\langle n_2 t_2 \sigma_\gamma(E) \rangle}$$

$$\doteq \frac{\left\langle \sigma_\gamma(E) e^{-n_1 t \sigma(E)} \right\rangle}{\langle \sigma_\gamma(E) \rangle}$$

$$\doteq \frac{\left\langle \sigma_\gamma(E) e^{-n_1 t [\sigma(E) + \langle \sigma \rangle - \langle \sigma \rangle]} \right\rangle}{\langle \sigma_\gamma(E) \rangle}$$

$$\doteq e^{-n_1 t \langle \sigma \rangle} \frac{\left\langle \sigma_\gamma(E) e^{-n_1 t [\sigma(E) - \langle \sigma \rangle]} \right\rangle}{\langle \sigma_\gamma(E) \rangle} \tag{B15}$$

Here again we can define the right-most term of equation (B15) to be a fluctuation correction ξ; that is,

$$\xi = \frac{\left\langle \sigma_\gamma(E) e^{-n_1 t [\sigma(E) - \langle \sigma \rangle]} \right\rangle}{\langle \sigma_\gamma(E) \rangle} \tag{B16}$$

$$\bar{S} \doteq e^{-n_1 t \langle \sigma \rangle} \xi \tag{B17}$$

Assuming a small fluctuation in the total cross section compared to $1/(n_1 t)$, we can expand the exponential as in (B13)

$$\xi = 1 - n_1 t \frac{\langle \sigma_\gamma(E) [\sigma(E) - \langle \sigma \rangle] \rangle}{\langle \sigma_\gamma(E) \rangle} \tag{B18}$$

The term ξ can be related to η, the fluctuation correction for transmission.

$$\xi = \frac{\left\langle \sigma_\gamma(E) e^{-n_1 t[\sigma(E)-\langle\sigma\rangle]} \right\rangle}{\langle \sigma_\gamma(E) \rangle} \tag{B19}$$

$$= \left[\frac{\left\langle \sigma_\gamma(E) e^{-n_1 t\sigma(E)} \right\rangle}{\langle \sigma_\gamma(E) \rangle \left\langle e^{-n_1 t\sigma(E)} \right\rangle} \right] \left[\left\langle e^{-n_1 t[\sigma(E)-\langle\sigma\rangle]} \right\rangle \right]$$

$$= \left[\frac{\left\langle \sigma_\gamma(E) e^{-n_1 t\sigma(E)} \right\rangle}{\langle \sigma_\gamma(E) \rangle \left\langle e^{-n_1 t\sigma(E)} \right\rangle} \right] \eta \tag{A20}$$

This then is the relation of η to ξ.

The average effective total cross section from the self-indication ratio is defined as

$$\left\langle (\sigma_t)_s \right\rangle = \frac{-1}{(n_1 t)} \ln \bar{S} \tag{A21}$$

Substituting from equation (B17)

$$\left\langle (\sigma_t)_s \right\rangle \doteq \frac{\langle\sigma\rangle - 1}{(n_1 t)} \ln (\xi) \tag{B22}$$

Now let us consider the expansion of ξ shown in equation (B18); the value of $\langle \sigma_\gamma(E)[\sigma(E) - \langle\sigma\rangle] \rangle$ is positive because the cross-section fluctuations are caused by the resonances. The positive contribution to this term where the capture cross section is near the peak of a resonance is greater than the corresponding negative contribution when the capture cross section is small; that is, far from the resonance peak. Thus, ξ should be smaller than 1.

$$\left\langle (\sigma_t)_s \right\rangle \doteq \frac{\langle \sigma \rangle - 1}{(n_1 t)} \ln \text{ (smaller than 1)}$$

$$\left\langle (\sigma_t)_s \right\rangle \doteq \langle \sigma \rangle + \text{Positive term}$$

$$\left\langle (\sigma_t)_s \right\rangle \geq \langle \sigma \rangle$$

Finally,

$$\left\langle (\sigma_t)_s \right\rangle \geq \langle \sigma \rangle \geq \langle \sigma_t \rangle \tag{B23}$$

or the true average total cross section is bracketed by the effective average total cross section determined by self-indication on the high side and that determined by transmission on the low side.

REFERENCES

1. Brissenden, R. J.; and Durston, C.: The Calculation of Neutron Spectra in the Doppler Region. Proceedings of the Conference on the Application of Computing Methods to Reactor Problems. Rep. ANL-7050, Argonne National Lab., 1965, pp. 51-76.

2. Bogart, Donald; and Semler, Thor T.: Monte Carlo Interpretation of Sphere Transmission Experiments for Average Capture Cross Sections at 24 keV. Neutron Cross Section Technology. AEC Rep. CONF-660303, Book 1, 1966, pp. 502-501.

3. Moore, M. S.; and Simpson, O. D.: Measurement and Analysis of Cross Sections of Fissile Nuclides. Conference on Neutron Cross Section Technology. AEC Rep. CONF-660303, Book 2, 1966, pp. 840-872.

4. Dyos, M. W.: Construction of Statistical Resonances in the Unresolved Resonance Region: The PSEUDO Code. Rep. GA-7136, General Dynamics Corp., May 26, 1966

5. Byoun, T. Y.; Block, R. C.; and Semler, T. T.: Temperature-Dependent Transmission and Self-Indication Measurements Upon Ta in the Unresolved Region. Conference on Neutron Cross Sections and Technology. AEC Rep. CONF-710301, Vol. 2, 1971, pp. 895-900.

6. Simpson, O. D.; and Miller, L. G.: A Technique to Measure Neutron Cross Sections in the Low keV Energy Region. Nucl. Instr. Methods, vol. 61, 1968, pp. 245-250.

7. Simpson, O. D.; and Miller, L. G.: Studies of Unresolved Resonances with a 2-keV Neutron Beam. Trans. Am. Nucl. Soc., vol. 11, no. 1, June 1968, pp. 298-300.

8. Semler, Thor T.: DAISY-An Efficient Program For Production of Neutron Pseudo Resonance Parameter Chains in the Unresolved Energy Region. NASA TN D-5837, 1970.

9. Wood, R. E.: Slow-Neutron Resonance Scattering in Ag, Au, and Ta. Phys. Rev., vol. 104, no. 5, Dec. 1, 1956, pp. 1425-1433.

10. Evans, J. E.; Kinsey, B. B.; Waters, J. R.; and Williams, G. H.: Radiation Widths of Neutron Resonances in Ta. Nucl. Phys., vol. 9, 1958/59, pp. 205-217.

11. Doil'nitsyn, Ya. A.; Kham'yanov, L. P.; and Parfenov, V. A.: Measurement of the Total Effective Cross Section Of Tantalum Using A Mechanical Neutron Selector. Proceedings of the Working Conference on Slow Neutron Physics. AEC-TR-5734, 1963, pp. 57-61.

12. Stolovy, A.: Neutron-Resonance Spin States in Ta and Re. Bull. Am. Phys. Soc., vol. 8, no. 1, Jan. 1963, p. 70.

13. Seth, K. K.; Hughes, D. J.; Zimmerman, R. L.; and Garth, R. C.: Nuclear Radii by Scattering of Low-Energy Neutrons. Phys. Rev., vol. 110, no. 3, May 1, 1958, pp. 692-700.

14. Divadeenam, Mundrathi: Strength Functions and the Optical Model. Ph.D. Thesis, Duke Univ., 1967.

15. Desjardins, J. S.; Rosen, J. L.; Havens, W. W., Jr.; and Rainwater, J.: Slow Neutron Resonance Spectroscopy. II. Ag, Au, Ta. Phys. Rev., vol. 120, no. 6, Dec. 15, 1960, pp. 2214-2226.

16. Garg, J. B.; Rainwater, J.; and Havens, W. W.: Neutron Total Cross Section Of Elements With Closely Spaced Levels In The Energy Region of 5 eV To About 10 keV. Paper 95 presented at the Conference on the Study of Nuclear Structure with Neutrons, Antwerp, 1965, p. 534.

17. Data of Garg, J. B.; Rainwater, J.; and Havens, W. W.: Neutron Cross Sections. Vol. IIC, Z = 61 to 87. Murrey D. Goldberg, Said F. Mughabghab, Surendra N. Purohit, Benjamin A. Magurno, and Victoria M. May, eds. Rep BUL-325, Second ed., Suppl. 2, Vol. IIC, Brookhaven National Lab., Aug. 1966, p. 73-181-12.

18. Simpson, O. D.; Fluharty, R. G.; and Shankland, R. S.: Neutron Strength Functions ($\overline{\Gamma}_n^0/\overline{D}$). Bull. Am. Phys. Soc., vol. 3, no. 3, May 1958, p. 176.

19. Seth, K. K.; Tabony, R. H.; Bilpuch, E. G.; and Newson, H. W.: s-, p-, And d-Wave Neutron Strength Functions. Phys. Letters, vol. 13, no. 1, Nov. 1, 1964, pp. 70-72.

20. Frike, M. P.; Mathews, D. R.; Friesenhan, S. J.; Carlson, A. D.; and Neill, J. M.: Radiative Capture Cross Sections for 1-1000 keV Neutrons. Conference on Neutron Cross Sections and Technology. AEC Rep. CONF-710301, Vol. 1, 1971, pp. 252-258.

21. Dilg, W.; and Vonach, H. K.: Average Total Neutron Cross Sections of Heavy Elements at 2.7 keV. Statistical Properties of Nuclei. J. G. Garg, ed., Plenum Press, 1972, pp. 327-334.

22. Canright, R. Bruce, Jr.; and Semler, Thor T.: Comparison of Numerical Techniques for the Evaluation of the Doppler Broadening Functions $\psi(x, \theta)$ and $\chi(x, \theta)$. NASA TM X-2559, 1972.

23. Kittel, Charles: Introduction to Solid State Physics. Second ed., John Wiley & Sons, Inc., 1956, p. 132.

24. Semler, Thor T.; and Riehl, John P.: Computer Program For Evaluation of Bloch-Grueneisen Parameters Of Metals And Evaluation Of Electrical Resistivity of Tantalum as a Function of Temperature. NASA TM X-2320, 1971.

25. Lamb, Willis E., Jr.: Capture of Neutrons by Atoms in a Crystal. Phys. Rev., vol. 55, no. 2, Jan. 15, 1939, pp. 190-197.

26. Dresner, Lawrence: Resonance Absorption in Nuclear Reactors. Pergamon Press, 1960, p. 33.

27. Semler, Thor T.: Effect of Multiple Spin Species on Spherical Shell Neutron Transmission Analysis. NASA TM X-2546, 1972. (To be published in Journal of Nucl. Energy.)

28. Semler, Thor T.: PREJUD-A Computer Code for the Preliminary Analysis of Two-Dimensional Pulse Height Analyzer Data. NASA TM X-2181, 1971.

29. Akima, Hiroshi: A New Method of Interpolation and Smooth Curve Fitting Based on Local Procedures. Assoc. Comp. Mach., vol. 17, no. 4, Oct. 1970, pp. 589-602.

30. Simpson, O. D.; Smith, J. R.; and Rogers, J. W.: Filtered-Beam Techniques. Conference on Flux Normalization and Cross Section Standards. AEC Rep. CONF-701002, 1970, pp. 362-376. (Especially p. 366.)

31. Simpson, O. D.; Smith, J. R.; and Rogers, J. W.: Neutron Filtered Beams as Standard Sources. Conference on Neutron Cross Sections and Technology. AEC Rep. CONF-710301, Vol. 2, 1971, pp. 598-604.

32. Block, R. C.; and Byoun, T. Y.: Linear Accelerator Project. Rep. RPI-328-187, Rensselaer Polytechnic Inst., Mar. 31, 1970, pp. 32-42.

33. Kannenberg, Robert G.: CINEMATIC-Fortran Subprograms for Automatic Computer Microfilm Plotting. NASA TM X-1866, 1969.

NASA-Langley, 1973 —— 22 E-7282

"The aeronautical and space activities of the United States shall be conducted so as to contribute . . . to the expansion of human knowledge of phenomena in the atmosphere and space. The Administration shall provide for the widest practicable and appropriate dissemination of information concerning its activities and the results thereof."

—NATIONAL AERONAUTICS AND SPACE ACT OF 1958

NASA SCIENTIFIC AND TECHNICAL PUBLICATIONS

TECHNICAL REPORTS: Scientific and technical information considered important, complete, and a lasting contribution to existing knowledge.

TECHNICAL NOTES: Information less broad in scope but nevertheless of importance as a contribution to existing knowledge.

TECHNICAL MEMORANDUMS: Information receiving limited distribution because of preliminary data, security classification, or other reasons. Also includes conference proceedings with either limited or unlimited distribution.

CONTRACTOR REPORTS: Scientific and technical information generated under a NASA contract or grant and considered an important contribution to existing knowledge.

TECHNICAL TRANSLATIONS: Information published in a foreign language considered to merit NASA distribution in English.

SPECIAL PUBLICATIONS: Information derived from or of value to NASA activities. Publications include final reports of major projects, monographs, data compilations, handbooks, sourcebooks, and special bibliographies.

TECHNOLOGY UTILIZATION PUBLICATIONS: Information on technology used by NASA that may be of particular interest in commercial and other non-aerospace applications. Publications include Tech Briefs, Technology Utilization Reports and Technology Surveys.

Details on the availability of these publications may be obtained from:

SCIENTIFIC AND TECHNICAL INFORMATION OFFICE

NATIONAL AERONAUTICS AND SPACE ADMINISTRATION

Washington, D.C. 20546